STUDY OF USING POZZOLANIC MATERIALS AS ADDITIVES FOR API CLASS G CEMENT

Watcharakon Setwong

A Thesis Submitted in Partial Fulfillment of the Requirements for the

Degree of Master of Engineering in Geotechnology

Suranaree University of Technology

Academic Year 2016

การศึกษาการใช้วัสดุปอซโซลานเป็นสารเติมแต่งสำหรับ เอพีไอ ซีเมนต์คลาสจี

นายวัชรากร เศษวงษ์

วิทยานิพนธ์นี้เป็นส่วนหนึ่งของการศึกษาตามหลักสูตรปริญญาวิศวกรรมศาสตรมหาบัณฑิต
สาขาวิชาเทคโนโลยีธรณี
มหาวิทยาลัยเทคโนโลยีสุรนารี
ปีการศึกษา 2559

STUDY OF USING POZZOLANIC MATERIALS AS ADDITIVES FOR API CLASS G CEMENT

Suranaree University of Technology has approved this thesis submitted in partial fulfillment of the requirements for a Master's Degree.

Thesis Examining Committee

(Prof. Dr. Kittitep Fuenkajorn)
Chairperson

(Asst. Prof. Dr. Akkhapun Wannakomol)
Member (Thesis Advisor)

(Asst. Prof. Dr. Bantita Terakulsatit)
Member

(Prof. Dr. Sukit Limpijumnong)
Vice Rector for Academic Affairs and Innovation

(Assoc. Prof. Flt. Lt. Dr. Kontorn Chamniprasart)
Dean of Institute of Engineering

:

(STUDY OF USING POZZOLANIC MATERIALS AS ADDITIVES FOR API CLASS G CEMENT) : .

, 107

10 15 20 30

80

7 28 50

20 50 80

15 20

สามารถช่วยเพิ่มความแข็งแรงในการต้านทานแรงกด และยังสามารถช่วยลดค่าความซึมซาบของตัวอย่างซีเมนต์แข็งได้อย่างมีประสิทธิภาพอีกด้วย

สาขาวิชา เทคโนโลยีธรณี ลายมือชื่อนักศึกษา อำพาภร

ปีการศึกษา 2559 ลายมือชื่ออาจารย์ที่ปรึกษา

WATCHARAKON SETWONG : STUDY OF USING POZZOLANIC MATERIALS AS ADDITIVES FOR API CLASS G CEMENT. THESIS ADVISOR : ASST. PROF. AKKHAPUN WANNAKOMOL, Ph.D., 107 PP.

FLY ASH/ PALM OIL FUEL ASH/ SUGARCANE BAGASSE ASH/ FILTRATE LOSS ADDITIVE

The main objective of research is to study the using of selected pozzolanic material, including fly ash (FLYA), palm oil fuel ash (POFA), and sugarcane bagasse ash (SCBA), as an additive of the oil well API Class G cement in order to lighten and improve the compressive strength and permeability property of the mixed cement. In this study cement slurry sample was replaced by each selected pozzolanic material at 10, 15, 20 and 30 by weight percent (wt%). The pozzolan cement slurry viscosity, density, filtrate loss volume and thickening time were measured. Some pozzolan cement slurry samples were used for marking set (solid) cement specimens. These set cement specimens were cured at room temperature and at 80°C with curing time of 7, 28, and 50 days. Results of measurement indicated that the viscosity of pozzolan cement slurry samples was not different significantly. It was also noticeable that the density and fluid loss volume of pozzolan cement slurry sample were reversely proportional to the amount of selected pozzolanic materials. The selected pozzolanic material could prolong the cement thickening time. Results of the set pozzolan cement samples measurements indicated that the compressive strength of set pozzolan cement specimens was directly proportional to the amount of mixed pozzolanic material and curing time due to the effect of pozzolanic reaction. It was found that when the set

cement was made from cement slurry mixed with more than 20 wt% of each selected pozzolanic material and the curing time of 50 days at 80°C its compressive strength decreased. This is because the amount of calcium hydroxide to pozzolanic reaction was reduced. The permeability of set pozzolan cement sample also decreased with increasing amount of pozzolanic materials and curing time. It can be concluded that the selected pozzolanic materials could be used as an oil well API class G cement additive if it is used to replace oil well API class G cement at range between 15-20 wt%. This is because with this replacement ratio the filtrate loss volume and viscosity of the cement slurry are not much different from those of the cement without pozzolanic material while the density is lowered. These selected pozzolanic materials can increase the compressive strength and can also reduce the permeability of the set cement specimens effectively.

School of Geotechnology

Academic Year 2016

Student's Signature Watcharakon

Advisor's Signature

ACKNOWLEDGEMENTS

I would like to express my appreciation to the thesis committee member, Prof. Dr. Kittitep Fuenkajorn, Asst. Prof. Dr. Akkhapun Wannakomol and Asst. Prof. Dr. Bantita Terakulsatit. I would like expresses special gratitude and appreciation to Asst. Prof. Dr. Akkhapun Wannakomol who assisted in the selection of thesis topic, effectively and patiently steered me to the right path. Finally, I most gratefully acknowledge my parents, everyone around me and all members of School of Geotechnology Institute of Engineering Suranaree University of Technology, for all their help and support throughout the period of this research.

Watcharakon Setwong

TABLE OF CONTENTS

Page

TABLE OF CONTENTS (Continued)

Page

TABLE OF CONTENTS (Continued)

Page

TABLE OF CONTENTS (Continued)

Page

TABLE OF CONTENTS (Continued)

Page

LIST OF TABLES

Table Page

LIST OF FIGURES

Figure Page

LIST OF FIGURES (Continued)

Figure Page

LIST OF FIGURES (Continued)

Figure Page

SYMBOLS AND ABBREVIATIONS

A	=	Cross-sectional area
BP	=	Barometric pressure
cc	=	Cubic centimeter
cP	=	Centipoises
CMCG	=	API class G cement
FLYA	=	Fly ash
g	=	Gram
k	=	Fluid consistency index
K	=	Permeability
L	=	Sample length
lb/gal	=	Pound per gallon
ml	=	Milliliter
mm	=	Millimeter
n	=	Flow behavior index
P	=	Inlet pressure
psi	=	Pound per square inch
POFA	=	Palm oil fuel ash
q	=	Flow rate
rpm	=	Rotational speed, (round per minutes)
SG	=	Specific gravity

SYMBOLS AND ABBREVIATIONS (Continued)

SEM	=	Scanning Electron Microscope
SCBA	=	Sugar cane bagasse ash
t	=	Time of bleed out
V_t	=	Volume of filtrate collected at the time of the bleed out
wt%	=	Percent by weight of binder material
W/B	=	Water per binder material ratio
XRD	=	X-ray Diffraction
XRF	=	X-ray Fluorescence
˚F	=	Degree Fahrenheit
˚C	=	Degree Celsius
τ	=	Shear stress
τ_0	=	Yield stress
τ_y	=	Yield point
μ	=	Viscosity
μ_a	=	Apparent viscosity
μ_p	=	Plastic viscosity
μm	=	Micrometer
γ	=	Shear rate
ϕ_{300}	=	Viscosity dial reading at 300 rpm
ϕ_{600}	=	Viscosity dial reading at 600 rpm
ϕ_i	=	Viscometer dial reading

CHAPTER I

INTRODUCTION

1.1 Rationale and background

In order to lighten and increase the cement compressive strength and permeability, some pozzolanic materials can be used as an additive for these purposes (Chindaprasirt et al., 2007). Pozzolanic material, e.g. fly ash, palm oil fuel ash, and sugarcane bagasse ash, is one of the cement additives in civil construction material in present day. Pozzolanic oil well cements are typically used to produce lightweight slurries because the specific gravity of the pozzolanic material is lower than that of the cement. A pozzolan slurry has a lighter weight than a corresponding Portland cement slurry of similar consistency. The lighter weight cement keeps the formation from breaking down especially in the sub normal pressure zone where. It is important not to exceed the fracture pressure of the formation while cementing.

Some pozzolanic materials also have a high water demand that effectively gives a higher yield and lighter slurry. They also tend to improve compressive strength over time (Sata et al., 2007). The additional binding material also reduces permeability and minimizes attack from formation waters. In most cases, pozzolanic materials can also reduce the effect of sulfate attack, though this is to a certain degree dependent on the slurry design. However, the appropriate mixing ratio of cement, pozzolanic material, and other binder materials is not well studied and determined.

Therefore, this study aims to determine the optimum material mixing ratio in order to improve the strength and permeability properties of the mixed cement slurry samples together with their rheology properties, fluid filtration loss, and thickening time, respectively. Some local and abundant pozzolanic material, including fly ash, sugarcane bagasse ash, and palm oil ash, were used in this study since they were wastes, low costs, and easy to provide locally.

1.2 Research objectives

The objectives of this study are to study the feasibility of using pozzolanic materials, including fly ash, palm oil fuel ash, and sugarcane bagasse ash, as an additive for API Class G cement and to determine the optimum mixing ratio of the API Class G Cement, pozzolanic materials, and other binder materials in order to lighten and improve the compressive strength and permeability property of the mixed cement.

1.3 Research methodology

The relevant literature from book, and previous works had been searched and reviwed. The summary of the literature review is given in the thesis. The colleted fly ash, palm oil fuel ash, and sugarcane bagasse ash were milled and passed sieve number 325. Then, each selected pozzolanic materials and API class G cement powder were chemical and physical properties test. In this study cement slurry sample were replaced by each selected pozzolanic materials at 10, 15, 20 and 30 wt%, and these pozzolan cement slurry viscosity, density, filtrate loss volume and thickening time were measured. Some pozzolan cement slurry samples were used for marking set

(solid) cement specimens. These set cement specimens were cured at room temperature and 80˚C with curing time of 7, 28, and 50 days, respectively. This research had been conducted in five main steps as showed in Figure 1.1. Detail of research methodology and measurements are given in chapter 3.

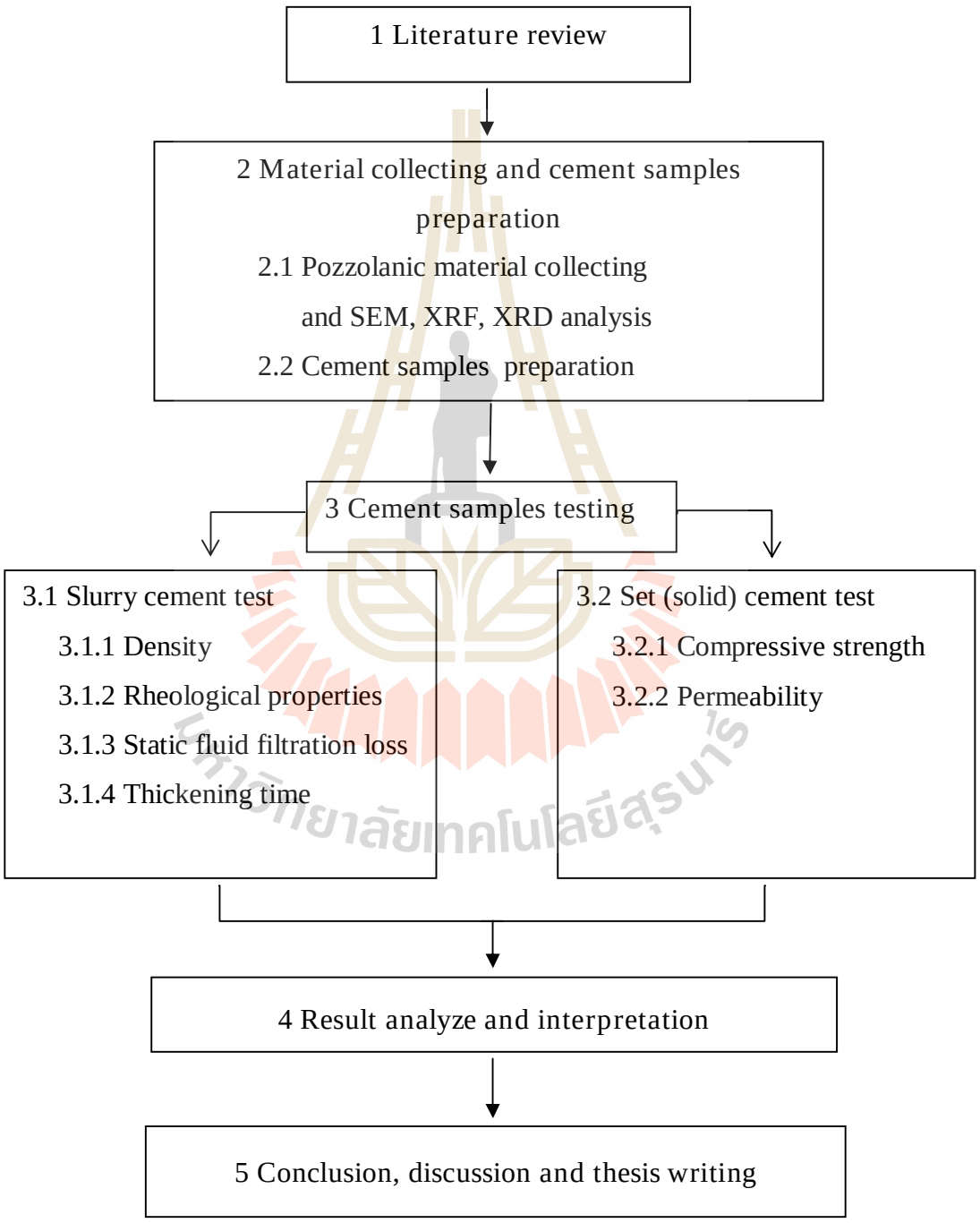

Figure 1.1 Flowchart showing the research methodology

1.4 Scope and limitation of the study

This study was focused on the properties of API Class G cement mixing with binder material were pozzolanic materials, including fly ash, palm oil fuel ash, and sugarcane bagasse ash which was ground by a ball milled until the ground sample particles passed a sieve number 325 (size 45 microns). The study is divided into two main parts, the first part is for the slurry cement test, including viscosity, density, thickening time, and fluid filtration loss determination. The second part is the compressive strength and permeability determination of the set (solid) cement specimens which are set at curing time of 7, 28 and 50 days under room temperature and 80°C.

1.5 Thesis contents

Chapter I introduces the background of research problem and rational, research objective, research methodology, and scope and limitations of the study, respectively. Chapter II summarizes the result of the literure review. Chapter III describes the sample preparations and test methods. Chapter IV describes and discusses the results from the laboratory experiments. Chapter V concludes the research results and gives some recommendations for the future experiments.

CHAPTER II

LITERATURE REVIEW

2.1 Introduction

This chapter summarizes the results of literature review which can be divided into seven main topics: (1) Cement in petroleum drilling industry, including cement chemical properties, cement physical properties and cement additives, (2) Formation pressure, (3) Pozzolan cement and pozzolanic reaction, (4) Fly ash (FLYA), (5) Palm oil fuel ash (POFA), and (6) Sugarcane bagasse ash (SCBA), respectively.

2.2 Cement in petroleum drilling industry

Most cement used in the petroleum industry is a type of Portland cement. Thomas and Alan (2006) explain this type of cement is used in well drilling for 5 purposes as;

(1) To isolate the hydrocarbon bearing formations from water bearing formations and one hydrocarbon bearing formation from another, i.e., gas and oil,

(2) To protect and secure the casing in the hole,

(3) To prevent caving of the hole,

(4) To provide a firm seal and anchor for the wellhead equipment, and

(5) To protect casing from corrosion by sulfate-rich formation waters, if exposed to direct contact with the casing.

Portland cement is produced from limestone and other materials (such as clay or shale) by heating at 2,600°F to 3,000°F (Thomas and Alan, 2006).

2.2.1 Cement chemical properties

Portland cement usually contains of two Oxide groups as;

(1) Major oxide: CaO, SiO_2, Al_2O_3, and Fe_2O_3 about 90% of the total weight of the cement.

(2) Minor oxide: MgO, Na_2O, K_2O, TiO_2, P_2O_5 and Gypsum.

Oxides which are components of Portland cement are shown in Table 2.1.

Table 2.1 Major and minor oxide components of Portland cement (modified after , 2548)

Oxide		Percent by weight
Major Oxide	CaO	60 - 67
	SiO_2	17 - 25
	Al_2O_3	3 - 8
	Fe_2O_3	0.5 - 6.0
Minor Oxide	MgO	0.1 - 5.5
	$Na_2O + K_2O$	0.5 - 1.3
	TiO_2	0.1 - 0.4
	P_2O_5	0.1 - 0.2
	SO_3	1 - 3

Major and minor oxides are assembled during clinking and 8 main compounds are then produced as shown in Table 2.2.

Table 2.2 Main compounds of major and minor oxide of Portland cement (modified after , 2548)

Main Compound		Chemical Composition	Abbreviation
Major Oxide	Tricalcium Silicate	$3CaO \times SiO_2$	C_3S
	Dicalaium Silicate	$2CaO \times SiO_2$	C_2S
	Tricalcium Aluminate	$3CaO \times Al_2O_3$	C_3A
	Tetracalcium Aluminoferrite	$4CaO \times Al_2O_3 \times Fe_2O_3$	C_4AF
Minor Oxide	Calcium Salphate Dihydrate (Gypsum)	$CaSO_4 \times 2H_2O$	-
	Free Lime	-	CaO
	Magnesium Oxide	-	MgO
	Alkali Oxides	-	Na_2O, K_2O

API basically divided cement into class A to class J (without class I). This classification of cement depends on depth and temperature of down hole conditions.

API Cement Classes (King, 2006)

Class A: For using from surface to 6,000 feet (1830 meter) depth when special properties are not required.

Class B: For using from surface to 6,000 feet (1,830 meter) depth when conditions require moderate to high sulfate resistance.

Class C: For using from surface to 6,000 feet (1,830 meter) depth when conditions require high early strength.

Class D: For using from 6,000 to 10,000 feet (1,830 to 3,050 meter) depth when under conditions of high temperatures and pressure.

Class E: For using from 10,000 to 14,000 feet (3,050 to 4,270 meter) depth when under conditions of high temperature and pressures.

Class F: For using from 10,000 to 16,000 feet (3,050 to 4,880 meter) depth when under conditions of extremely high temperatures and pressures.

Class G: Intended for using as basic cement from surface to 8,000 feet (2,440 m) depth. This can be used with accelerators and retarders to cover a wider range of well depths and temperatures. Cement that use in this thesis is in this class.

Class H: A basic cement for using from surface to 8,000 feet (2,440 meter) depth as manufactured. This can be used with accelerators and retarders to cover a wider range of well depths and temperatures.

Class J: Intended for using as manufactured from 12,000 to 16,000 feet (3,600 to 4,880 meter) depth when under conditions of extremely high temperatures and pressures. It can be used with

accelerators and retarders to cover a range of well depths and temperatures.

2.2.2 Cement physical properties

Portland cements are commonly characterized by their physical properties for quality control purposes. Their physical properties can be used to classify and compare Portland cements. The challenge in physical property characterization is to develop physical tests that can satisfactorily characterize key parameters, including compressive strength and pump ability time.

2.2.2.1 Compressive Strength

Compressive strength of neat cement increases over the period of several weeks. The compressive strength of particular time during the curing process depends heavily on mixing and curing conditions. Typical compressive strength of API Class G cement during various curing conditions is shown in Table 2.3.

Compressive strength is one of the properties used to test the reliability of cementing and is the ability of a material to withstand deformation when load is applied. Compressive strength of a cement concrete depends on the type of raw materials including additives used, mixture proportions, concrete structure, method and time of curing, and exposure conditions (Herianto and Fathaddin, 2005).

2.2.2.2 Pump ability time

Pump ability time or thickening time of cement slurry is an important factor in slurry design. Generally these statements can be made regarding

thickening time. Some conclusions on pump ability time and temperature, pressure, and water content are listed as follows.

- Higher the temperature – faster the set. This is a primary factor affecting thickening time.

- Higher the pressure – faster the set. This effect is more pronounced below 5000 psi, but continues up through limits of lab test equipment.

- Loss of water from slurry accelerates set.

- Shutdown during placement results in cement gelation which will shorten pump ability and accelerate set and strength development.

Table 2.3 Typical compressive strength of API class G cement during various curing conditions (after Thomas and Alan, 2006)

Curing conditions		24-hour compressive strength, psi
Temp (°F)	Pressure (psi)	
80	0	615
60	0	1,470
95	800	2,085
110	1,600	2,925
140	3,000	5,050
170	3,000	5,920

The effect of temperature on thickening time of API class G cement is presented in Table 2.4.

Table 2.4 Relations between thickening time and temperature of API class G cement (modified after Thomas and Alan, 2006)

Circulating Temperature (°F)	Thickening Time (hours : minute)
91	4:00+
103	3:36
113	2:25
125	1:40

2.2.3 Cement and additives

The raw ingredients of Portland cement are lime, silica, alumina and iron oxide. Today's well cements have to resist a big range of well depths and conditions. In permafrost zones, the cement must resist below-freezing condition, while in thermal recovery wells or geothermal fields they must endure temperatures above 350°C (660°F). In petroleum drilling industry have varied conditions, cement can be formulated by using additives. Cement additives which number more than 100 and are used for different profits. However cement additives can be grouped into 8 major categories as follows:

1. Accelerators: reduce cement setting time and speed up the development of compressive strength. They are commonly used in shallow, low temperature wells.

2. Retarders: extend cement setting time and allow sufficient time for slurry placement in deep wells.

3. Extenders: reduce cement density and may also reduce the amount of cement needed for a job. Low-density cement is needed for cementing weak formations which would otherwise breakdown and cause lost circulation.

4. Weighting agents: increase cements density. These are used for cementing high-pressure formation which might become unstable if slurry density were too low.

5. Dispersant: reduce the viscosity of cement slurry and ensure good mud removal during placement.

6. Fluid-loss control agents: control water loss from the cement into the formation.

7. Lost – circulation control agents: reduce the loss of cement slurry into weak or muggy formations. Loss of cement may necessitate a costly, remedial cementing operation.

8. Special additives such as antifoam agents and fibers are manufactured for specific cementing tasks, such as the prevention of foaming that might lead to a loss in hydraulic pressure (Mitchell, 2006).

2.3 Formation Pressure

When a well is drilled, the natural state of the rock formations is disrupted. The wellbore creates a disturbance where only the formations and their natural forces existed before. During the planning stages of a cement job, certain information must be known about the formations, e.g. Pore pressure, Fracture pressure and Rock

characteristics. Generally, these factors will be determined during drilling. The density of the drilling fluids in a properly balanced drilling operation can be a good indication of the limitations of the wellbore.

To maintain the integrity of the wellbore, the hydrostatic pressure exerted by the cement, drilling fluid, etc. must not exceed the fracture pressure of the weakest formation. The fracture pressure is the upper safe pressure limitation of the formation before the formation breaks down (the pressure necessary to extend the formation's fractures). The hydrostatic pressures of the fluids in the wellbore, along with the friction pressures created by the fluid movement, cannot exceed the fracture pressure, or the formation will break down. If the formation does break down, the formation is no longer controlled, and lost circulation results. Lost circulation, or fluid loss, must be controlled for successful primary cementing. Pressures experienced in the wellbore also affect the strength development of the cement (Society of Petroleum Engineers, 2015).

In many parts of the world, lost circulation and weak formations with low fracture gradients are common. These situations require usually the low-density cement system to reduce the hydrostatic pressure of the fluid column during cement placement. Consequently, lightweight additives (also known as extenders), are used to reduce the weight of the cement slurry (Mitchell, 2006) in order to avoid a rock formation from breaking down while cementing in subnormal pressure condition. In this study the pozzolanic materials were tested and used as a cement extender additive.

2.4 Pozzolanic cement and pozzolanic reaction

2.4.1 Pozzolanic cements

Pozzolanic materials include any natural or industrial siliceous or silicon-aluminous material, which will be combined with lime in the presence of water at ordinary temperatures to produce strength-developing insoluble compounds similar to those formed from hydration of Portland cement. Typically, pozzolanic material is categorized as natural or artificial, and can be either processed or unprocessed. The most common sources of natural pozzolanic materials are volcanic materials and DE. Artificial pozzolanic materials are produced by partially calcining natural materials such as clays, shale, and certain siliceous rocks, or are more usually obtained as an industrial by-product. Artificial pozzolanic materials include metakaolin, fly ash, microsilica (silica fume), and ground granulated blast-furnace slag.

Mitchell (2006) has written explained pozzolanic oil-well cements are typically used to produce lightweight slurries. Because the specific gravity of the pozzolanic material is lower than that of the cement, pozzolan slurry has a lighter weight than corresponding Portland cement slurry of similar consistency. The lighter weight keeps the formation from breaking down. It is important not to exceed the fracture pressure of the formation while cementing. Some pozzolanic materials also have a high water demand that effectively gives a higher yield and lighter slurry. They also tend to improve compressive strength over time. The additional binding material also reduces permeability and minimizes attack from formation waters. In most cases, pozzolanic materials can also reduce the effect of sulfate attack, though this is to a certain degree dependent on the slurry design (Awal and Hussin, 1997).

2.4.2 Pozzolanic reaction

A pozzolan is a material that is made up of silicon dioxide (SiO_2), aluminum oxide (Al_2O_3), and ferric oxide (Fe_2O_3) as the main components and, when the oxides of these three are combined, it will not be lower than 50 % of the total mass of water; there may be little or no binder, but after the milling process it can react with calcium hydroxide ($Ca(OH)_2$) which is a product from the hydration reaction. The hydration reaction is the reaction of cement when it reacts with water. This reaction produces the compound of calcium silicate hydrate (C-S-H), calcium aluminate hydrate (C-A-H), ettringite, and calcium hydroxide ($Ca(OH)_2$). Calcium hydroxide from the hydration reaction also reacts with SiO_2 and Al_2O_3 in pozzolanic material and provides a compound of C-S-H and C-A-H, respectively. These two reactions are called the pozzolanic reaction. However, the pozzolanic reaction is limited by the amount of SiO_2, Al_2O_3, and $Ca(OH)_2$ from the hydration reaction of the cement (Serametjakun, 2001).

2.5 Fly ash

Fly ash is by far the most widely used of the pozzolanic materials. Fly ash (FLYA), generated during the combustion of coal for energy production, is an industrial by-product which is recognized as an environmental pollutant. The fly ash is generally grey in color, abrasive, mostly alkaline, and refractory in nature. There are very small size from ranging 1-200 micrometers and also contains different essential elements, including both macronutrients P, K, Ca, Mg and micronutrients Zn, Fe, Cu, Mn, B, and Mo for plant growth. Ahmaruzzaman (2010) reported that the fly ash from pulverized coal combustion was used for mixing in Portland pozzolan

cement. This pozzolan are siliceous or siliceous and aluminous materials that together with water and calcium hydroxide form Cementitious products at ambient temperatures are also admixtures. The geotechnical properties of fly ash (e.g., specific gravity, permeability, internal angular friction, and consolidation characteristics) make it suitable for use in construction.

2.5.1 Fly ash type

According to ASTM Standard C618, there are three types of fly ash: Class F, Class C, and Class N based on the performance of different fly ashes. ASTM Standard C618 classifies fly ashes on the basis of the combined percentages of SiO_2 + Al_2O_3 + Fe_2O_3 (Table 2.5). There is a much greater relationship between CaO content and performance. The CaO content ranges from 2 or 3 to 30% by weight of the fly ash. The "true" Class F fly ash has a CaO content of less than 10%, whereas a "true" Class C has CaO greater than 20%. Fly ashes having CaO between 10 and 20% behave somewhat differently from either the true Class F or Class C. Fly ash are generally composed of amorphous glassy particles that are spherical in shape.

Table 2.5 Fly ash classification based on composition (wt%) (after ASTM C 618, 2001)

Properties	Class		
	N	F	C
Silicon dioxide (SiO_2) plus aluminum oxide (Al_2O_3) plus iron oxide (Fe_2O_3), min, %	70.0	70.0	50.0
Sulfur trioxide (SO_3), max, %	4.0	5.0	5.0
Moisture content, max, %	3.0	3.0	3.0
Loss on ignition, max, %	10.0	6.0**	6.0

Class N is natural pozzolanic and class C is fly ash (by product) of lignite and sub-bituminous.

** The use of Class F pozzolanic containing up to 12% loss on ignition may be approved by the user if either acceptable performance records or laboratory test results are made available.

2.5.2 Fly ash in oil well cement

Mitchell (2006) suggested that the ASTM Class F fly ash is the most common used in oil well cementing. The major advantages of the Class F fly ash are its low cost and abundance worldwide. The performance characteristics of a Class F fly ash vary little from batch-to-batch from a given source. However, the differences between sources can be considerable because the composition can vary from the true low CaO to 10 to 20% CaO. This produces significant variations in performance characteristics. Therefore, Class F fly ashes from different source should be tested before using. Specific gravities also must be determined. Some power plants produce Class F fly ashes with high carbon content because of poor burning. These should be avoided for oil well cementing because they can cause severe gelation problems. The

use of Class C fly ash as an extender for well cementing is relatively limited. This is, in part, because of the limited availability of Class C fly ash and the considerable variability that exists not only between sources, but also to a large extent between batches from a given source.

Halliburton (2003) reported that the properly mixed slurry containing micro fly ash cement component will showed no appreciable viscosifying or gelation and reduced the required amount of retarder. Slurries containing micro fly ash cement component exhibit improved resistance to sulfate attack and better response to conventional lignosulfonate retarders. At temperatures below 230°F (110°C), micro fly ash cements component helps control strength retrogression. Slurries containing micro fly ash cement component exhibit superior compressive strength and penetration abilities.

2.6 Palm oil fuel ash

Malaysia, Indonesia, and Thailand are amongst the countries in the equatorial belt that cultivate oil palm and palm oil products. The palm oil industry is one of the major agro-industries in Thailand. Palm oil fuel ash is a by-produced in palm oil industry. After palm oil is extracted from the palm oil fruit, both palm oil husks and palm oil shell are burned as fuel in the boiler of palm oil mill. The burning process results in an ash, which is referred as palm oil fuel ash (POFA). After combustion in the steam boiler, about 5% POFA by weight of solid wastes is produced (Sata et al., 2004). The ash produced sometimes varies in tone of color from whitish grey to darker shade based on the carbon content in it. POFA causes a nuisance to the environment. Since the tropical countries are continuously increasing the production

of palm oil, the quantity of POFA is also increasing and thus creating a large environmental load (Abdullah et al., 2006). Due to the absence of sufficient nutrients required for a fertilizer, POFA is mostly dumped in open field near palm oil mills without any profitable return, thus causing environmental pollution and health hazard (Sumadi and Hussin, 1995; Tonnayopas et al., 2006).

2.6.1 Properties of palm oil fuel ash

2.6.1.1 Physical properties

The physical properties of POFA are greatly influenced by the burning condition, particularly burning temperature (Abdullah et al., 2006). A number of physical properties of unground and ground POFA used in various studies are shown in Table 2.6.

Table 2.6 Physical properties of POFA (modified Safiuddin et al., 2011)

Properties	Unground POFA	Ground POFA
Color	Light grey/whitish	Dark grey
Specific gravity	1.78 - 1.97	2.22 - 2.78
Median particle size, d_{50} (μm)	54.3 - 183	7.2 - 10.1
Mass passing through 45μm sieve (%)	5.6 - 58.8	97 - 99
Specific surface area (m^2/kg)	796	882 - 1244

Color: Generally, unground POFA is light grey in color. This is due to the unburned carbon content left at relatively low burning temperature. The unburned carbon content becomes very low when the burning temperature is high.

Unground POFA can be whitish in the absence of unburned carbon (Abdullah et al., 2006). The color becomes dark grey in case of ground POFA.

Specific gravity: The specific gravity of unground POFA generally varies in the range of 1.78-1.97. After the grinding process, the specific gravity of POFA increases and is found to be in the range of 2.22-2.78 (Sata et al., 2004; Tangchirapat et al., 2009). This is because the grinding process decreases the porosity with reduced particle size.

Particle shape and size: The particle shape and size of ground and unground POFA are different. From scanning electron microscopy, it was found that the unground POFA particles are mostly large, spherical and porous. In contrast, the ground POFA generally consists of crushed particles with irregular and angular shape. The median particle size (d_{50}) of unground POFA varies in the range of 54.3-183 μm. After grinding, the median particle size of POFA can be reduced to 7.2-10.1 μm (Sata et al., 2004; Chindaprasirt et al., 2008).

Fineness: The particle size of POFA can be reduced by the grinding process in ball mills (Sata et al., 2007; Tangchirapat et al., 2007; Tangchirapat et al., 2009). POFA may also be ground in a Los Angeles abrasion machine using mild steel bar (12 mm diameter and 800 mm long) instead of steel ball (Abdullah et al., 2006; Awal and Hussin, 1999; Hussin and Awal, 1996). The grinding process reduces not only the particle size, but also the porosity of POFA (Kiattikomol et al., 2001). After grinding, POFA can be less porous with smaller particles (Paya et al., 1996).

The fineness of POFA can also be expressed with regard to the percent mass passing through or retained on sieve number 325 (45 μm). The percent

mass passing sieve number 325 can be in the range of 5.6-58.8% for unground POFA whereas it can be 97-99% for ground POFA. Both specific surface area and percent mass passing sieve number 325 reveal that the surface area of POFA becomes higher after grinding.

2.6.1.2 Chemical composition

The major chemical component of POFA is SiO_2, which varies in the range of 44-66 wt%. The other pozzolanic components are Al_2O_3 and Fe_2O_3. The loss on ignition (LOI) and SO_3 are in the range of 0.1-21.5 wt% and 0.2-3 wt%, respectively (Table 2.7). There are many arguments in justifying the classification of POFA based on its chemical composition. This is possibly due to the variability in the nature of product, and also because of various burning conditions. Hence, more study is needed to avoid this contradiction by establishing a proper classification.

Table 2.7 Chemical composition of POFA (after Safiuddin et al., 2011)

Chemical components	Weight fraction (%)
SiO_2	44 - 66
Al_2O_3	1.5 - 11.5
Fe_2O_3	1.5 - 5.5
$SiO_2 + Al_2O_3 + Fe_2O_3$	55 - 70
CaO	4 - 8.5
MgO	2 - 6.5
K_2O	2 - 8.5
Na_2O	0.1 - 3.5
SO_3	0.2 - 3.0
Loss on ignition (LOI)	0.1 - 21.5

2.6.2 Palm oil fuel ash in cement

The study of palm oil fuel ash was started by Tay (1990) who used it to replace Portland cement with 10-50 wt%. He found that in the range of 20-50 wt% of cement replacement, the decrease in the compressive strength of concrete at various ages was almost proportional to amount of the ash in the concrete mixtures, except when only 10 wt% ashes was used. Later, Awal and Hussin (1997) reported that palm oil fuel ash had a good potential in suppressing expansion due to sulfate attack. In 2004, it was found that palm oil fuel ash, which contained a substantial amount of silica and was ground to a suitable fineness, could be used as a pozzolanic material to

produce high strength concrete as high as 100 MPa at 90 days (Sata et al., 2004).

In Thailand, Sukantapree et al., (2002) revealed that the compressive strength of mortar containing original POFA was low due to the large particle size and high porosity of POFA. However, mortar containing ground POFA (GPOFA) with particles retained on a 45 μm sieve (Number 325) of 4.3% gave a compressive strength higher than 100% of control mortar at the curing ages of 7 and 28 days. Furthermore, a previous investigation (Sata et al., 2004) indicated that POFA with high fineness has a highly pozzolanic reaction and can be used as a supplementary cementation material for producing high strength concrete.

Tangchirapat et al. (2003) reported the results revealed that the replacement of POFA in Portland cement increased setting time of paste. For constant flow of 105-115, the mortar mixed with POFA required higher water than that of standard mortar. After grinding, the use of ground POFA reduced setting time as compared to that of unground POFA paste and decreased water requirement. However, mortars with ground POFA (d_{50} = 19.9 and 10.1 microns) at 20 wt% of cement replacement gives the compressive strength higher than 75% of standard mortar at the age of 7 and 28 days. In addition, the use of 10 and 20 wt% of high fineness POFA (d_{50} = 10.1 microns) gives higher compressive strength of mortar than that of standard mortar and it is 104 and 101 wt%, respectively at the age of 90 days. The results suggest that the ground POFA can be used as a good pozzolanic material.

Kroehong et al. (2012) reported the blended cement pastes containing 20% of POFA with high fineness had the lowest total porosity. The $Ca(OH)_2$ contents of blended cement paste containing POFA decreased with the increasing replacement of POFA and they were lower than those of the Ordinary Portland cement (OPC)

cement paste. In addition, the critical pore size of blended cement paste containing POFA was lower than that of the OPC cement paste. The incorporation of high fineness POFA into cement paste decreased the critical pore size of blended cement paste more than that with coarse POFA.

2.7 Sugarcane bagasse ash

Sugarcane is one of the foremost crops grown in all over countries. After the extraction of all economical sugar from sugarcane, about 40-45% fibrous residue is obtained. It is reused in the same industry as fuel in boilers for heat generation leaving behind 8-10% ash as waste, known as sugarcane bagasse ash (SCBA) (Modani and Vyavhare, 2013). At present, SCBA waste is ultimately disposed of as soil fertiliser in many sugarcane-producing countries. However, this option has three disadvantages: (1) it causes significant changes in the physical-chemical properties of soils, (2) it contributes to environmental pollution, and (3) it may have a strong negative impact on human health. Thus, the SCBA waste production presents a serious waste management problem for the sugarcane industry (Schettino and Holanda, 2015).

2.7.1 Properties of sugarcane bagasse ash

The sugarcane bagasse consists of approximately 50 wt% of cellulose, 25 wt% of hemicelluloses of lignin. Each ton of sugarcane generates approximately 26% of bagasse (at a moisture content of 50%) and 0.62 wt% of residual ash (Srinivasan and Sathiya, 2010). The residue after combustion presents a chemical composition dominated by silicon dioxide (SiO_2). The chemical and physical properties are given in Table 2.8 and Table 2.9, respectively.

Table 2.8 Chemical composition of SCBA (after Cordeiro et al., 2004)

Chemical components	Weight fraction (%)
SiO_2	78.34
Al_2O_3	8.55
Fe_2O_3	3.61
CaO	2.15
Na_2O	0.12
K_2O	3.46
MnO	0.13
TiO_2	0.5
MgO	1.65
BaO	< 0.16
P_2O_5	1.07
Loss on ignition (LOI)	0.42

Table 2.9 Physical properties of SCBA (modified Cordeiro et al., 2004; Madurwar et al., 2014; Tijore et al., 2013; Sivakumar et al., 2014)

Properties	SCBA
Color	gray-black
Specific gravity	2.20 - 2.40
Median particle size, d_{50} (μm)	28.9 - 45
Mass passing through 45-μm sieve (%)	8.4
Specific surface area (m^2/kg)	308 - 514
Density (g/cm^3)	2.16 - 2.52
Particle shape	Spherical

2.7.2 Sugarcane bagasse ash in cement

Chusilp et al., (2009) examined the importance of bagasse ash for development as pozzolanic materials in concrete. The physical properties of concrete containing ground bagasse ash (BA) including compressive strength, water permeability, and heat evolution were investigated and all tests were done in accordance with American Standards (ASTM). When bagasse ash is ground up into small particles, the compressive strength of concrete containing this ground bagasse ash improves significantly. The low water permeability values of concretes containing ground bagasse ash at 90 days were mostly caused by the pozzolanic reaction. The higher the replacement fraction of Portland cement by ground bagasse ash, the longer the delay time to obtain the highest temperature rise. Concrete containing up to 30% ground bagasse ash had a higher compressive strength and lower water permeability

than the control concrete, both at ages of 28 and 90 days.

All of the pastes containing bagasse ash showed normal consistency higher than the control paste. Higher replacement of cement by bagasse ash resulted in higher normal consistency because bagasse ash had high porosity. At the same replacements, use of ground bagasse ash as a partial replacement of cement in paste produced normal consistency lower than that of the original ash (Isaia, Gastaldini and Moraes, 2003).

Abbasi and Zargar (2013) studied the moisture percent and the method of burning bagasse, physical characteristics, chemical composition by XRF (X-ray florescence) and crystal fixtures by XRD (X-ray diffraction) test and specific area of bagasse ash and compared with cement. The burning of bagasse will produce very viscous smoke that causes difficulties for producers and near residential. Replacing cement by 10% of bagasse ash, their compressive strength at 28 days was increased by 25% in comparison with normal concrete specimens. Use of bagasse ash in concrete as 10% cement replacement causes slump increase and compressive strength and delayed in initial and final setting time. As per American Standards the above mentioned tests were conducted.

Srinivasan and Sathiya (2010) studied chemical and physical characterization of SCBA, and partially replaced in the ratio of 0, 5, 15, and 25% by weight (wt%) of cement in concrete. Compressive strength, split tensile strength, flexural strength and modulus of elasticity at the age of 7 and 28 days was obtained as per Indian Standards. It was found that the cement could be advantageously replaced with SCBA up to a maximum limit of 10 wt%. Therefore, it is possible to use sugarcane bagasse ash (SCBA) as cement replacement material to improve quality

and reduce the cost of construction materials such as concrete.

Somna and Jaturapitakkul (2011) explained the suitable replacement of ground bagasse ash to obtain the good long-term compressive strength, low water permeability, and high chloride resistance of recycled aggregate concrete was 20% by weight of binder material. The use of ground bagasse ash to partially replace cement could improve water permeability of recycled aggregate concrete to be lower than that of conventional concrete about 2-3 times.

CHEPTER III

RESEARCH METHODOLOGY

3.1 Introduction

This chapter describes basic characteristic of tested materials in this study which are pozzolanic material including fly ash, palm oil fuel ash, sugarcane bagasse ash and well drilling cement (API class G cement), cement slurry and set (solid) preparation, specimens measurement and testing, respectively.

3.2 Material collecting and cement samples preparation

3.2.1 Pozzolanic material collecting and analysis

3.2.1.1 Materials

API class G cement (CMCG), intended for use as basic cement from surface to 2,500 meter depth as manufactured, was selected for the experiments in this study. Selected pozzolanic materials including fly ash (FLYA), palm oil fuel ash (POFA), and sugarcane bagasse ash (SCBA) were ground by ball mill and sieved through sieve number 325 to get the particles size smaller than 45 microns.

3.2.1.2 Chemical and physical analysis

X-ray fluorescence (XRF) : The XRF technical are use the principles of that when X-rays high energy are incident to the specimen, and then specimen emit photons out (Fluoresced) toward the photons are emitted from different elements of specimen and have a specific wavelength (Energy) for each elements. Therefore, type of elements contained in specimen can be indicated by its specific wave length. The quantity of photons emitted depends on the amount of elements in specimen. This data can be analyzed to determine the amount of each element.

X-ray diffraction (XRD) : XRD is a technique that uses X-rays to analyze the compounds are presented in the sample and reveal a detailed study on crystal structure of the sample. XRD technique uses shooting a known wavelength of X-rays to incident the specimen and the diffraction angle of radiation are measured and recorded by receptor. The angle of diffraction of X-rays is depended on the composition and structure of the substance contained in the sample. This data can indicate type of compounds that are presented in the sample and can be used to study the details of crystal structure of the sample. In addition, data can also be used to determine the amount of each compound in the sample together with intensity, size, and integrity of crystal and the stress of compounds in the samples.

Scanning electron microscope (SEM) : SEM can show the surface characteristics of the material, size and shape of the powder particles. The positions of interest on specimen, demonstrate the nature and distribution of in-phase microstructure. A scanning electron microscope (SEM) is a type of electron microscope that produces images of a sample by scanning it with a focused beam of electrons. The electrons interact with atoms in the sample, producing various signals

that contain information about the sample's surface topography and composition. The electron beam is generally scanned in a raster scan pattern, and the beam's position is combined with the detected signal to produce an image. SEM can achieve resolution better than 1 nanometer. Specimens can be observed in high vacuum, in low vacuum, in wet conditions (in environmental SEM), and at a wide range of cryogenic or elevated temperatures.

The most common SEM mode is detection of secondary electrons emitted by atoms excited by the electron beam. The number of secondary electrons that can be detected depends, among other things, on specimen topography. By scanning the sample and collecting the secondary electrons that are emitted using a special detector, an image displaying the topography of the surface is created.

Samples for SEM can be solid, bulk specimens of any size that will fit within the specimen chamber. Samples are generally mounted rigidly on a specimen holder called a specimen stub using a conductive adhesive, but mechanical clamping is a possible alternative.

Nonconductive specimens tend to charge when scanned by the electron beam, and especially in secondary electron imaging mode, this causes scanning faults and other image artifacts. For conventional imaging in the SEM, specimens must be electrically conductive, at least at the surface, and electrically grounded to prevent the accumulation of electrostatic charge. Metal objects require little special preparation for SEM except for cleaning and mounting on a specimen stub. Non-conducting materials are usually coated with an ultrathin coating of electrically conducting material, deposited on the sample either by low-vacuum sputter coating or by high-vacuum evaporation. Conductive materials in current use

for specimen coating include gold, gold/palladium alloy, platinum, osmium, iridium, tungsten, chromium, and graphite. Coating with heavy metals may increase signal/noise ratio for samples of low atomic number (Z). The improvement arises because secondary electron emission for high-Z materials is enhanced.

3.2.2 Cement samples preparation

CMCG was partially mixed with FLYA, POFA, and SCBA at 10, 15, 20, and 30 wt%. The amount of selected pozzolanic materials mixing with water for all cements mixtures and cement mixer equipment shown in Figure 3.1. In this study, cement setting according to API standard. Cement slurry specimens were prepared for density, viscosity, fluid filtration loss, and thickening time measurement, respectively.

Figure 3.1 Cement mixer equipment (Kitchen Aid Professional 600)

Set (solid) cement specimens were then prepared from each selected pozzolan cement slurry sample in cubic shape size 2x2x2 inches (Figure 3.2a) and in cylindrical shape size $1^1/_2$ inches diameter and 2 inches length (Figure 3.2b). These set cement samples were cured at 7, 28, and 50 days. The cubic shape set cement sample were test for their compressive strength while the cylindrical shape set cement samples were tested their permeability.

Figure 3.2 Set (solid) cement sample a. is concretes cubic size 2x2x2 inches, b. are concretes cylinder

3.3 Cement specimen measurement and test methods

3.3.1 Density

The densities of cement slurry containing FLYA, POFA and SCBA at 10, 15, 20, and 30 wt% were measured at room temperature and at 80°C using the fluid density balance cup as shown in Figure 3.3. Each pozzolan cement slurry sample was filled in pressurized fluid density beam balance apparatus below the edge of cup. Placed the lid on the cup and check valve must be in open position. Then used the pressurized pump filled slurry up the cup until it was full. Placed the instrument on the knife edge and slides balanced weight right or left until the beam was balanced. Read and recorded specific gravity of cement slurry at the balance point.

Figure 3.3 Pressurized fluid density balance (Fann model 141)

3.3.2 Rheological properties

Viscosity of pozzolan cement slurry samples was measured by the viscometer as showed in Figure 3.4. The pozzolan cement slurry sample was filled in the viscometer cup below the edge of cup. The apparent viscosity (μ_a), plastic viscosity (μ_p) and yield point (γ_p) were calculated from 300 and 600 rpm reading according to equation 3.1, 3.2 and 3.3 respectively.

Figure 3.4 Viscometer (Fann model 35SA)

$$\mu_a = \phi_{600} / 2 \quad (3.1)$$

$$\mu_p = \phi_{600} - \phi_{300} \quad (3.2)$$

$$\gamma_p = \phi_{300} - \mu_p \quad (3.3)$$

where: ϕ_{600} is the viscosity dial reading at 600 rpm

ϕ_{300} is the viscosity dial reading at 300 rpm

μ_a is the apparent viscosity, (cP)

μ_p is the plastic viscosity, (cP)

γ_p is the Yield point, ($lb_f/100\ ft^2$)

The shear stress (τ) is determined as a function of the shear rate (γ). The shear stress and shear rate of pozzolan cement slurry samples were then calculated by using equation 3.4 and 3.5 respectively

$$\tau = 1.0678\phi_i \quad (3.4)$$

$$\gamma = 1.703 \times rpm \quad (3.5)$$

where: τ is the shear stress, ($lb_f/100ft^2$)

γ is the shear rate, (sec^{-1})

ϕ_i is the viscometer dial reading

rpm is the rotational speed, (round per minutes)

The power law model's parameters in the term of behavior index (n) and consistency (k) can be calculated from viscometer reading by equations (3.6) and (3.7).

$$n = 3.322\log(\phi_{600}/\phi_{300}) \quad (3.6)$$

$$k = 510\phi_{300}/511^{n} \quad (3.7)$$

where: n is the flow behavior index

k is the fluid consistency index

ϕ_{600} is the viscosity dial reading at 600 rpm

ϕ_{300} is the viscosity dial reading at 300 rpm

3.3.3 Static fluid filtration loss

Static fluid filtration loss of pozzolan cement slurry in this study was measured by the filtration test apparatus as showed in Figure 3.5. The Fluid filtration loss test was performed according to API RP-10B and some of them was based on standard API filter press test in which double layer screen 325 mesh on top and support screen 60 mesh were used as the filtration area. Cement slurry was full filled in the test cell of the apparatus. Pressure 100 psi was applied to the cell and recorded the filtrate volume for 30 second, 1 minutes, 2 minutes, 5 minutes, 7 minutes, 10 minutes, 15 minutes, 25 minutes, and 30 minutes, respectively. If bleed out occurred before 30 minute, recorded the filtrate volume and time at which the bleed out occurred and calculated the ISO fluid loss by using equation (3.8).

Figure 3.5 Filtration test apparatus (Fann model 821)

$$\text{ISO fluid loss} = V_t \frac{10.944}{\sqrt{t}} \quad (3.8)$$

where:

V_t is the volume of filtrate collected at the time of the bleed out, (milliliters)

t is the time of bleed out, (minutes)

If the test could be run entire 30 minutes without bleed out, measured the filtrate volume, doubled the value and reported it as the fluid loss value.

3.3.4 Thickening (setting) time

Thickening (setting) time of pozzolan cement slurry samples was measured by Vicat apparatus as showed in Figure 3.6. Cement slurry was filled in mold, removed the excess gently and made a smooth upper surface. Immediately after leveling the slurry, transferred mold and base-plate to the Vicat apparatus (use needle diameter of 1 millimeter.). Lower the needle until it contacts to surface of slurry, pause in that position 1-2 seconds, then recorded value after released the needle 30 seconds and repeated the test after 15 minutes to the same specimen and wait until needle penetrated to 25 millimeters, recorded initial setting time (total time after mixed). Final setting time was the total time after cement sample were mixed until needle penetrated only 0.5 millimeter into specimen.

Figure 3.6 Vicat apparatus

3.3.5 Compressive strength

Compressive strength of the set pozzolan cement samples was measured by the direct load compressive strength machine as showed in Figure 3.7. The set pozzolan cement in cubic shape size 2x2x2 inches cured in water at room temperature and 80°C until reach the testing ages of 7, 28, and 50 days. The specimens were compressed slowly and consistently until it failures. The unit of compressive strength is psi.

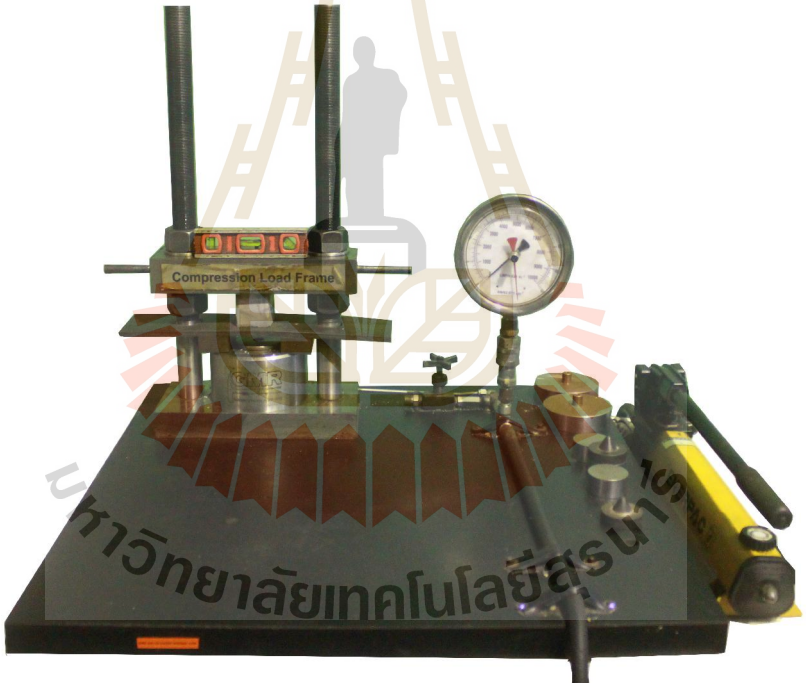

Figure 3.7 Direct load compressive strength machines

3.3.6 Permeability.

Permeability of set pozzolan cement in cylindrical shape size 1.5 inches diameter and 2 inches length was measured by Permeameter as showed in Figure 3.8. The set pozzolan cement sample was addressed in the sample core tube and the sample core tube was full filled with the liquid and then gas was injected. Once a stabilized flow rate was established, recorded the Upstream pressure (P, psi), Over burden pressure (BP, psi), Flow volume (cm^3), flow time (second), Barometric pressure (atm), and temperature (celcius) from instrument. The injected gas permeability (K_{gas}) can then be calculated by using Darcy's Law as presented in equations (3.9) and (3.10).

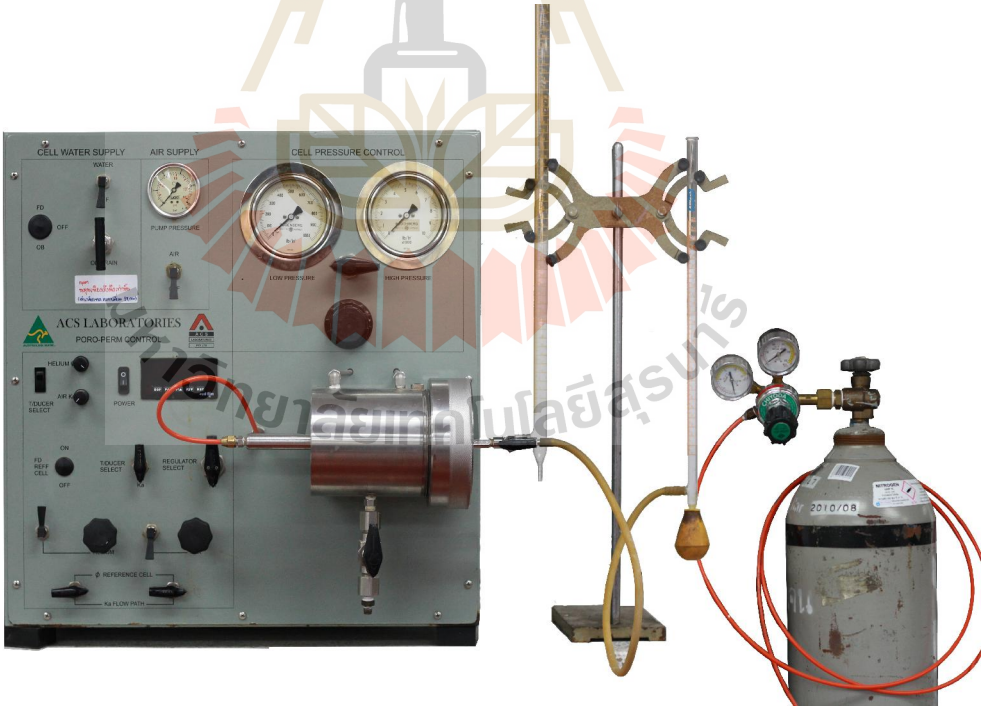

Figure 3.8 Permeameter (ACS laboratories)

$$K_{gas} = \frac{2000 \cdot BP \cdot \mu \cdot q \cdot L}{\left[\left(P_i \cdot 0.06805 + BP\right)^2 - \left(BP\right)^2\right] \cdot A} \quad (3.9)$$

$$K_{gas(actual)} = K_{gas} \times 0.9716 \quad (3.10)$$

where:

K	is the permeability, (md)
q	is the flow rate, (cc/sec)
μ	is the gas viscosity, (cp)
L	is the sample length, (cm)
A	is the cross-sectional area, (cm^2)
P	is the inlet pressure, (psig)
BP	is the barometric pressure, (atm)
0.06805	is conversion factor for psi to atmosphere
0.9716	is conversion factor for the expansion of air due to saturation with water vapor in the bubble tube

CHAPTER IV

RESULTS AND DISCUSSIONS

4.1 Introduction

This chapter describes the results of laboratory experiments which were used to determine chemical properties, physical properties, rheological properties, and cost comparison between cement, cement additive and cement mixed with pozzolanic material that used in petroleum well drilling respectively.

4.2 Chemical properties

4.2.1 X-ray fluorescence (XRF)

FLYA, POFA, and SCBA samples were analyzed their chemical compound and the results by X-ray fluorescence spectrometer. The chemical compositions in Table 4.1 reveals that the SCBA and the FLYA can be assigned as class F and class C pozzolan as prescribed by ASTM C 618 respectively. The POFA cannot be classified as any class of pozzolan according to ASTM C 618 standard because the contents of SiO_2 +Al_2O_3 + Fe_2O_3 were less than 50%. It should be noted that among of FLYA, POFA and SCBA the SiO_2 contents were rather different as 10.73 %, 17.07 %, and 44.85 %, respectively.

Table 4.1 Chemical compositions of cement and selected pozzolanic materials

Chemical composition (percentage)	CMCG	FLYA	POFA	SCBA
MgO	1.96	1.60	5.84	2.45
Al_2O_3	1.21	5.07	0.38	3.60
SiO_2	4.49	10.73	17.07	44.85
SO3	0.55	0.59	4.21	0.08
K_2O	0.27	2.63	38.81	6.30
CaO	86.61	28.40	23.78	11.53
TiO_2	0.29	0.04	0.40	2.69
Fe_2O_3	4.46	50.43	8.61	27.46
MnO_2	0.15	0.51	0.90	1.04
SiO_2+Al_2O_3+Fe_2O_3	-	66.23	26.06	75.91

4.2.2 X-ray diffraction (XRD)

The XRD tests in this study had been conducted in two main pasts. The first part was for FLYA, POFA, SCBA and API class G cement (CMCG) powder and the second part was 20 wt% pozzolan mixed ratio for set cement specimens of 28 days curing time at room temperature test, respectively.

Results of the XRD analysis revealed that the major mineral composition of FLYA, POFA, SCBA, and CMCG were Sylvite (KCl), Maghemite-C (Fe_2O_3), Quartz (SiO_2), Calcium sulfate ($CaSO_4$), Tricalcium silicate (Ca_3SiO_5) and Tricalcium aluminate ($Ca_3Al_2O_6$) and A=Arcanite (K_2S0_4). It was also found that the essential composition of selected pozzolan was Quartz, whereas Tricalcium silicate

and Tricalcium aluminate were essential composition of API cement class G. Result of the XRD analysis is depicted graphically in Figure 4.1.

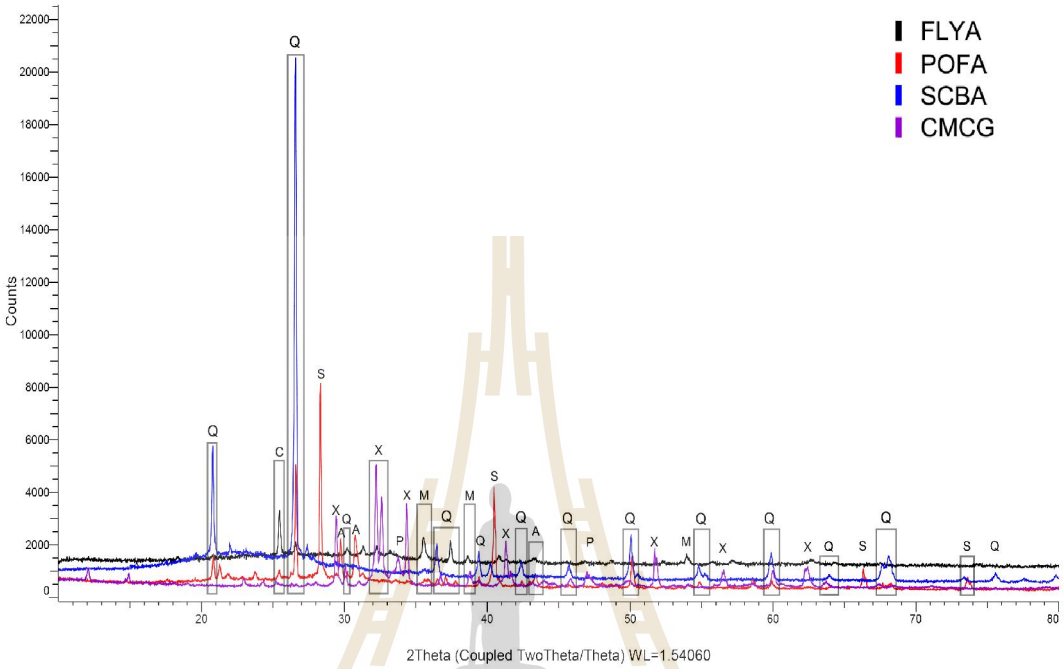

Note: S=Sylvite (KCl), M=Maghemite-C (Fe_2O_3), Q=Quartz (SiO_2), C=Calcium sulfate ($CaSO_4$), A=Arcanite (K2S04), and X= Tricalcium silicate (Ca_3SiO_5) and Tricalcium aluminate ($Ca_3Al_2O_6$).

Figure 4.1 Result of the XRD analysis of FLYA, POFA, SCBA, and CMCG dried power samples

For the second part test, result of the XRD analysis indicated that the mineral composition of the pozzolan set cement specimens were Ettringite, Portlandite, Quartz, Cadmium tellurate, and Calcium silicate hydrate. It is noticeable that quartz is still an essential mineral in all pozzolan set cement specimens as it is in all pozzolan cement paste samples. Moreover, portlandite and ettringite are found the most abundant only in the set cement specimens of CMCG.

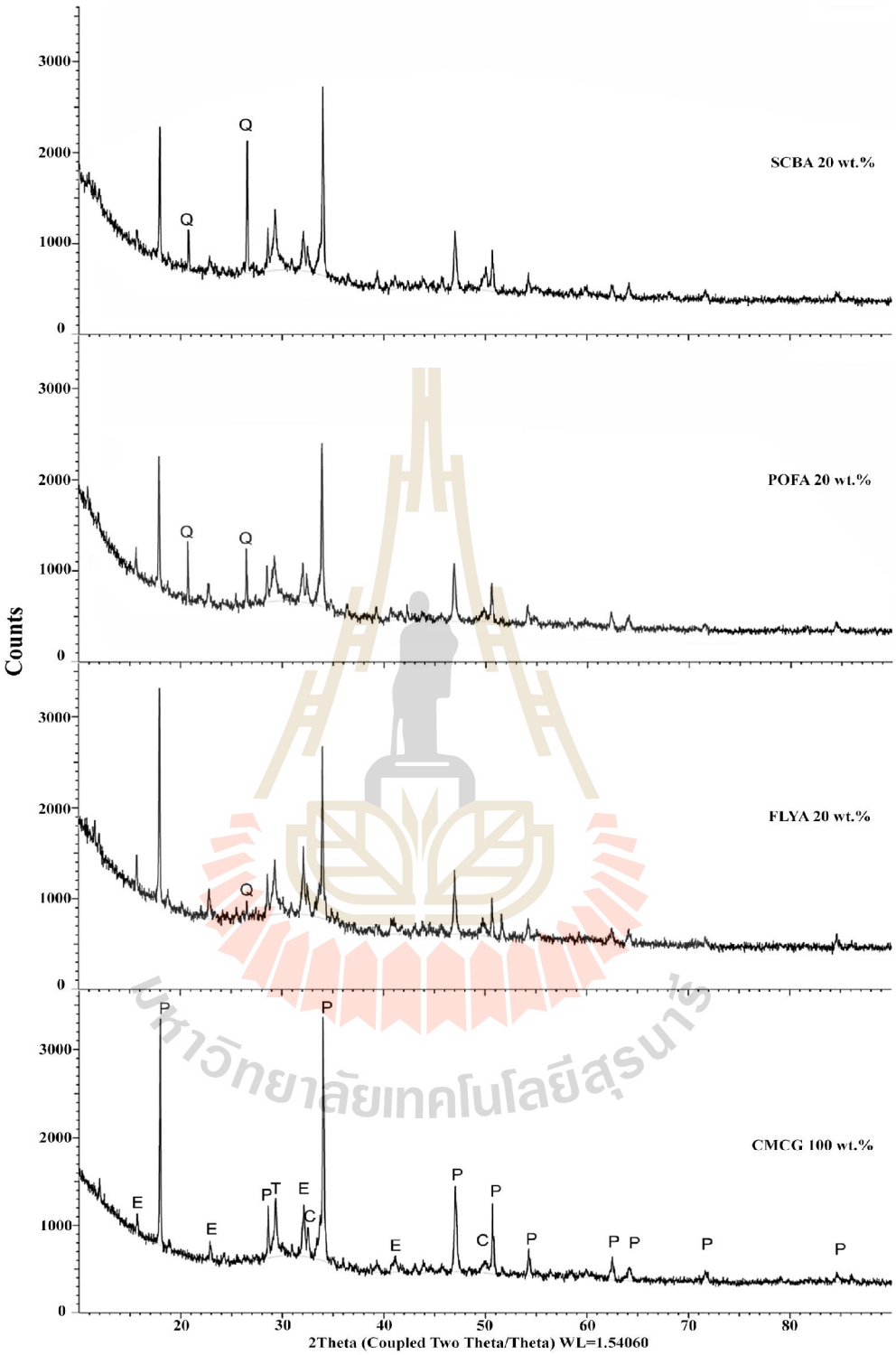

Note: E=Ettringite, P=Portlandite, Q=Quartz, T=Cadmium tellurate, C=Calcium silicate hydrate

Figure 4.2 Results of the XRD analysis of 20 wt% SCBA, POFA, FLYA mixed ratios and CMCG set cement curing at 28 days and room temperature

4.3 Physical properties

Basic physical property of dried of FLYA, POFA, SCBA, and CMCG power including specific gravity, particle shape, grain size distributions and water requirement for mixing were measured. Moreover, density, rheological properties, fluid filtration loss volume, thickening time, compressive strength and permeability of API class G cement and selected pozzolan cement were also measured in this study. Cement slurry samples were mixed by water-to-binder (W/B) ratios at about 0.5 and each selected pozzolanic material was added by 0, 10, 15, 20, and 30 wt% for these measurements, respectively.

4.3.1 Specific gravity and color of selected pozzolanic materials

Dried samples of FLYA, POFA, SCBA, and CMCG were sieved pass the sieve number 325 to get the dried sample size smaller than 45 µm. These sieved FLYA, POFA, SCBA, and CMCG samples were the measured their specific gravity measurement and color observation are showed in Table 4.2. It was found that specific gravity of CMCG was the highest (3.19) and followed by FLYA (2.54), POFA (2.27), and SCBA (2.08), respectively.

Table 4.2 Specific gravity and color of selected pozzolanic material

Materials	Specific gravity (SG)	Color
CMCG	3.19	Dark grey
FLYA	2.54	Brown
POFA	2.27	Light grey
SCBA	2.08	Black

4.3.2 Particle shape of selected pozzolanic materials

Dried powder sample of FLYA, POFA, SCBA, and API class G cement (CMCG) were ground by ball mill and sieved through the sieve mesh number 325 to get the dried size smaller than 45 μm. Sieved and unsieved dried powder of FLYA, POFA, SCBA, and CMCG were studied and observed their particle shape under the scanning electron microscope (SEM). Pictures of these dried pozzolanic materials and API class G cement powder are depicted in Figure 4.3.

Under SEM dried CMCG powder shows very small in size and irregular in shape compared to other samples (Figure 4.3a). The particle shape of FLYA is spherical with very round and smooth surface both in sieved and unsieved particle (Figure 4.3b and c). Some large pore can be observed at the surface of the large FLYA particles (Figure 4.3b). Most of POFA particle show rather spherical in shape, while some of them show elongate shape. They show irregular surface both in sieved and unsieved particle (Figure 4.3d and e). Some small pores can be observed on the large particle surface. Particle shape of SCBA is quite different between the unsieved and sieved particle. Unsieved particles still show the plant- tissue like structure with lots of large pores (Figure 4.3f). Sieved particles of SCBA show various type of shape including sphere, tabulate and fibrous (Figure 4.3g).

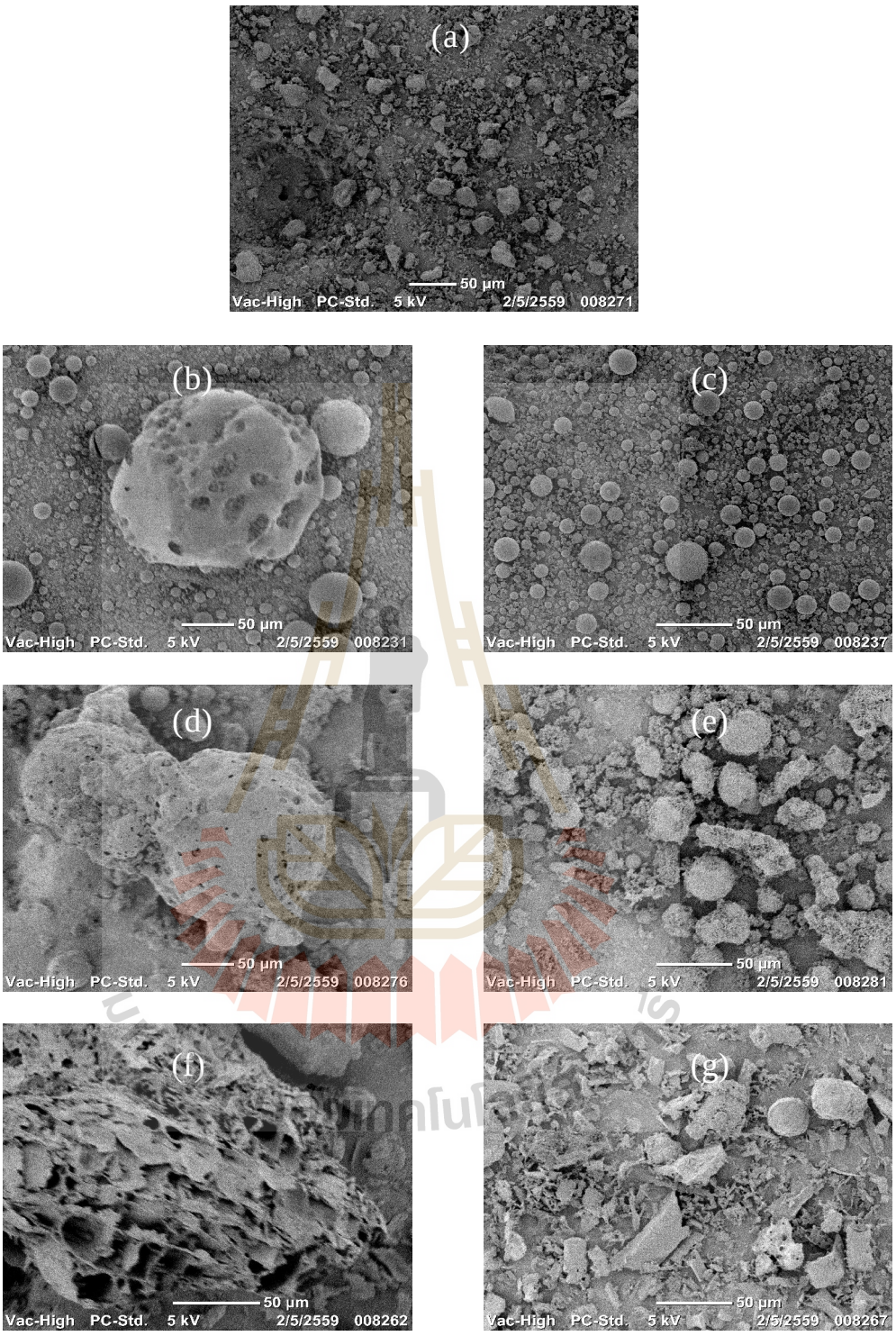

Figure 4.3 Particle of dried CMCG, FLYA, POFA, and SCBA powder under SEM: (a) = CMCG, (b) = FLYA, (c) = FLYA (<45µm), (d) = POFA, (e) = POFA (<45µm), (f) = SCBA, (g) = SCBA (<45µm)

4.3.3 Particle size distribution of selected pozzolanic materials

Particle size distribution of sieved FLYA, POFA, SCBA, and CMCG power was studied by Laser diffraction particle size distribution analyzer. Result of particle size distribution analysis is graphically presented in Figure 4.4. It was observed that the mean particle size of POFA is the biggest (25.29 µm) and followed by SCBA (20.45 µm), FLYA (12.75 µm), and CMCG (10.77 µm), respectively.

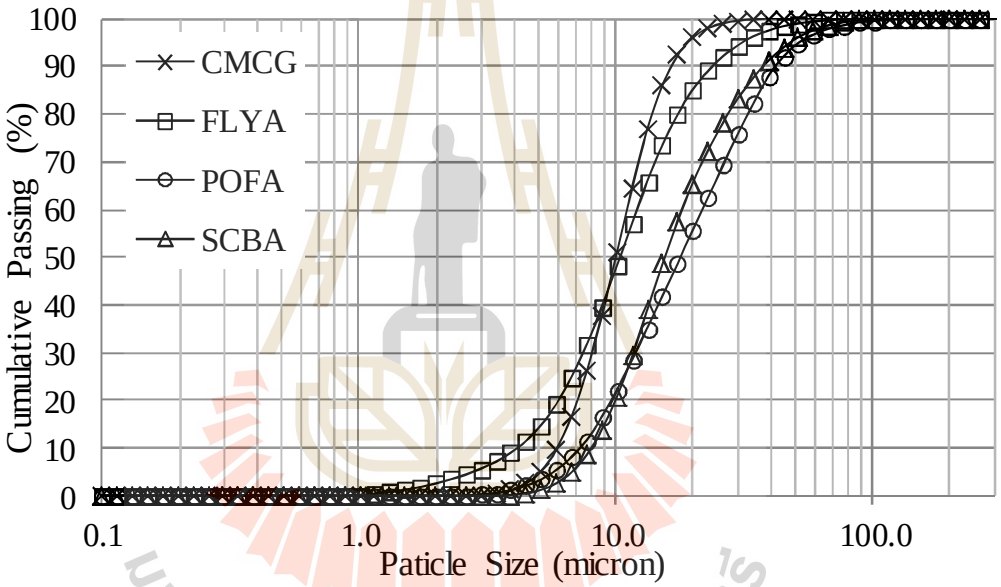

Figure 4.4 Particle size distributions

4.3.4 Water requirement for pozzolan cement slurry mixing

The amounts of water required for mixing the water-to-binder (W/B) ratios equal to 0.5 for each selected pozzolanic material at 10, 15, 20, and 30 wt% cement replacement are shown in Table 4.3. These pozzolan cement slurry sample were then measured their density, rheological properties, fluid filtration loss volume, and thickening time later on.

Table 4.3 Mixture properties of cement slurry

Mixtures	CMCG (g)	FLYA (g)	POFA (g)	SCBA (g)	Water (ml)	W/B
CMCG	1500				750	0.500
FLYA10	1350	150			750	0.500
FLYA15	1275	225			750	0.500
FLYA20	1200	300			750	0.500
FLYA30	1050	450			750	0.500
POFA10	1350		150		750	0.500
POFA15	1275		225		750	0.500
POFA20	1200		300		750	0.500
POFA30	1050		450		750	0.500
SCBA10	1350			150	750	0.500
SCBA15	1275			225	750	0.500
SCBA20	1200			300	750	0.500
SCBA30	1050			450	750	0.500

4.4 Pozzolan cement slurry test

4.4.1 Density

Density of the pozzolan cement slurry samples in this study was measured by Pressurized fluid density balance. The type of pozzolanic material has a different specific gravity (SG) with is affected to density of cement slurry. The SG of every selected pozzolanic material was lower than SG of the CMCG. Following the density measurement, the higher pozzolanic material mixed ratio, the lower density of

pozzolan cement slurry. Results of FLYA, POFA, and SCBA pozzolan cement slurry density measurement at various replacement wt% and at room temperature and 80˚C are showed in Table 4.4 and Figure 4.5 to Figure 4.7, respectively.

Table 4.4 FLYA, POFA, and SCBA pozzolan cement slurry density at 10, 15, 20, and 30 wt% mixed measured at room temperature and 80˚C

Mixed wt%	FLYA (lb/gal)		POFA (lb/gal)		SCBA (lb/gal)	
	Room temperature	80°C	Room temperature	80°C	Room temperature	80°C
0	15.39	15.47	15.39	15.47	15.39	15.47
10	15.17	15.37	15.12	15.28	15.00	15.10
15	15.06	15.25	14.81	15.09	14.83	14.98
20	14.91	15.10	14.65	14.94	14.47	14.65
30	14.62	14.74	14.56	14.72	13.97	14.37

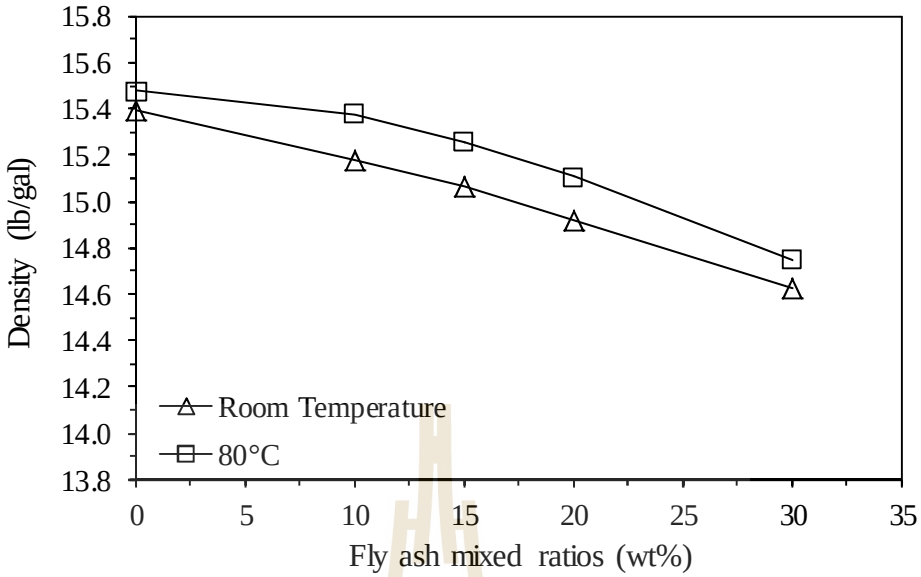

Figure 4.5 Results relation density and FLYA mixed ratios

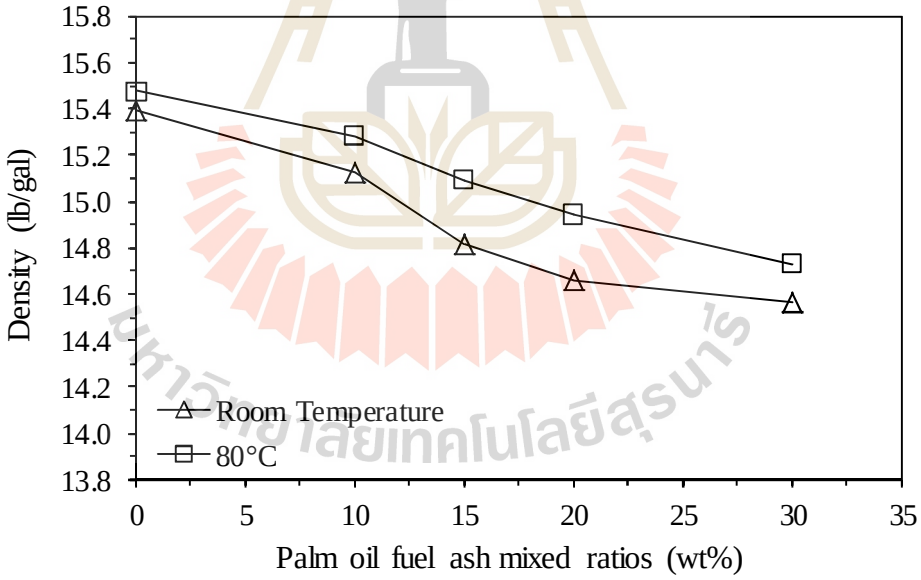

Figure 4.6 Results relation density and POFA mixed ratios

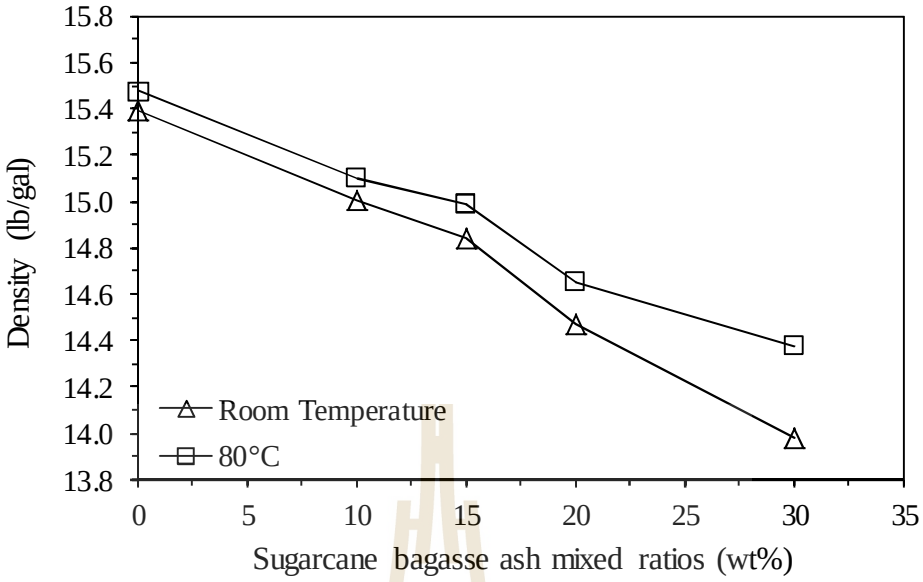

Figure 4.7 Results relation density and SCBA mixed ratios

It can be observed from Figure 4.5 to Figure 4.7 that the density of FLYA, POFA, and SCBA pozzolan cement slurry decreased with the increasing of amount of FLYA, POFA, and SCBA at the same temperature. It also found that when the temperature was elevated e.g. from room temperature to 80˚C, the density of all pozzolan cement slurry samples was increased. This is because of the vaporization loss of the mixing water has been occurred during the temperature is elevated. Among the selected pozzolan cement slurry, FLYA pozzolan cement slurry has the highest density and followed by POFA and SCBA pozzolan cement slurry, respectively.

4.4.2 Rheological properties of pozzolan cement slurry

Shear rate (γ), shear stress (τ), apparent viscosity (μ_a), plastic viscosity (μ_p), and yield point (γ_p) of pozzolan cement slurry, which were CMCG mixed by

selected pozzolanic materials at 10, 15, 20, and 30 wt% and at 0.5 W/B were measured in this study. Results of the measurement are as follows.

The shear stress and shear rates values for all six viscometer reading of API class G cement. The average viscometer readings were used to calculate the shear stress and shear rates by following equations (3.1) and (3.2) in previous chapter. The calculated the shear stress were plotted against shear rates in order to choose the best fit curve for the Power's law or Bingham plastic model. As a result, each plot curve was fitted with both linear and power equations. A correlation coefficient was obtained for each fitting curve. However, the Bingham plastic fluids were better fitted with a linear correlation, while the Power's Law fluids were fitted with power equations. For example, Figures 4.8 and 4.9 show the consistency plots for CMCG at room temperature and 80˚C. From the two plots, it can be inferred that the fluid is tend to be a Bingham Plastic fluid.

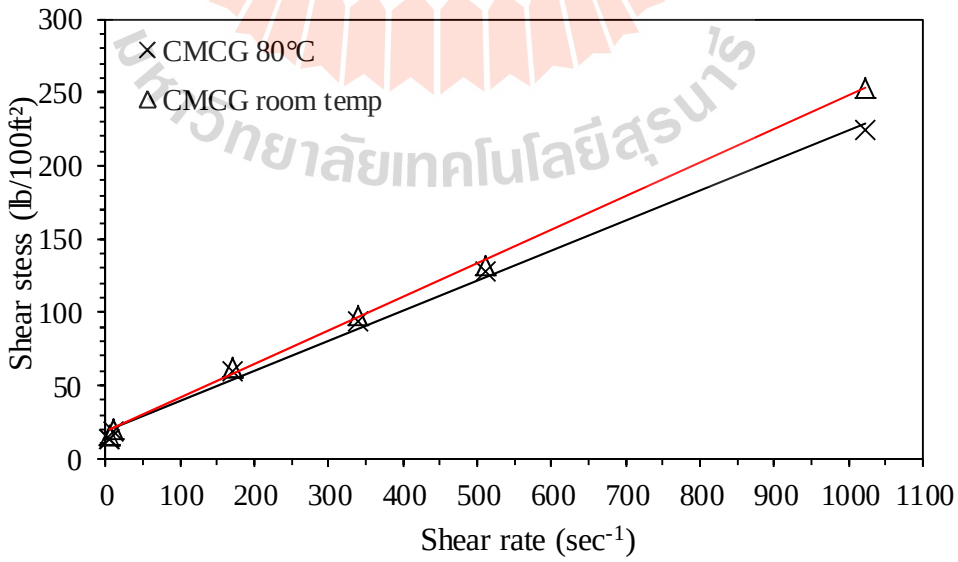

Figure 4.8 Consistency plot of CMCG with a linear correlation

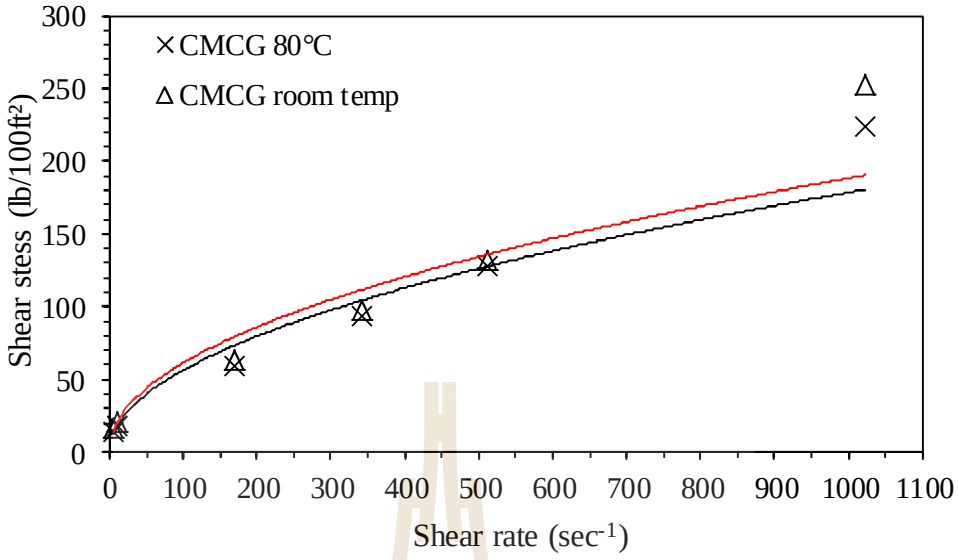

Figure 4.9 Consistency plot of CMCG with a power correlation

The appropriate rheological model for all other mixed cement slurry samples was determined in similar way. Their consistency curves were plotted as showed in Figures 4.10 through 4.15. On the plots, all cement slurry samples of FLYA and POFA tested at room temperature condition exhibited Bingham Plastic behavior but Power's Law behavior presented after elevated treatment temperature to 80˚C. It can be seen that FLYA and POFA containing cement slurry behaved both of behavior depending on temperature. SCBA cement slurry samples tested at room temperature and 80˚C condition exhibited only Bingham plastic model which is similar to CMCG. However, in this study it cannot exactly match the flow property of fluid with either the Bingham Plastic or Power's Law model. This is because most of oil well cement demonstrates the flow behavior in between the Bingham Plastic and the Power's Law model. Therefore, the rheological properties of cement slurry were

calculated for both models. Both models were used for cement slurry just for the comparison purposes.

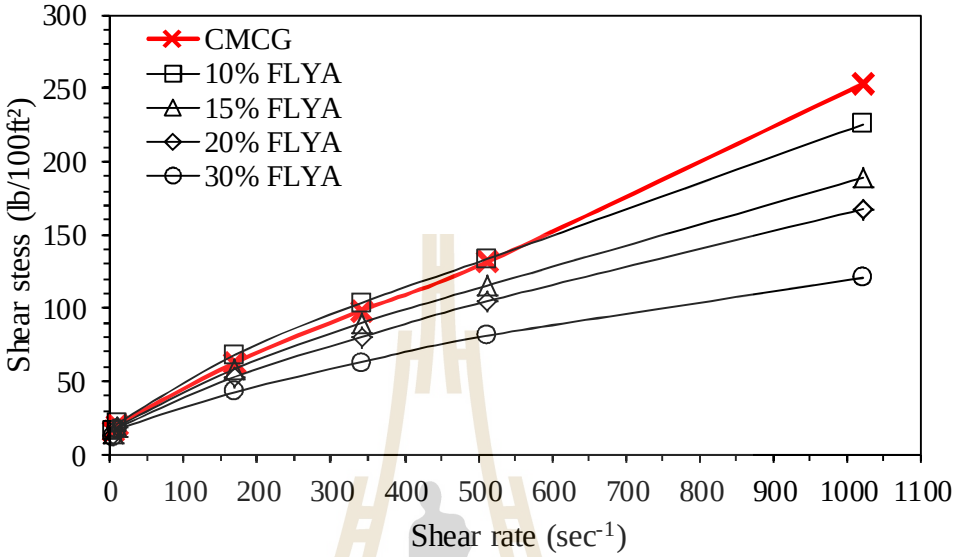

Figure 4.10 Consistency plot of FLYA at room temperature

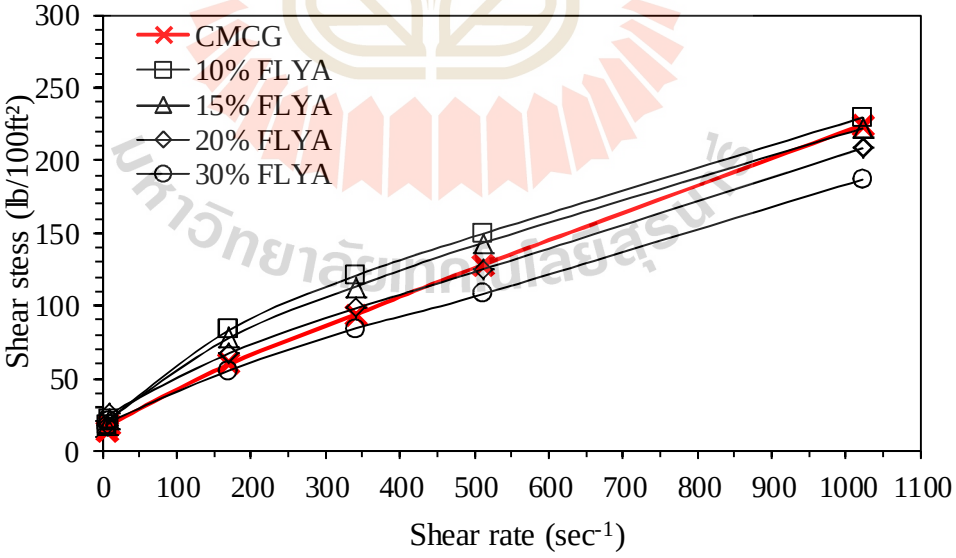

Figure 4.11 Consistency plot of FLYA at 80˚C

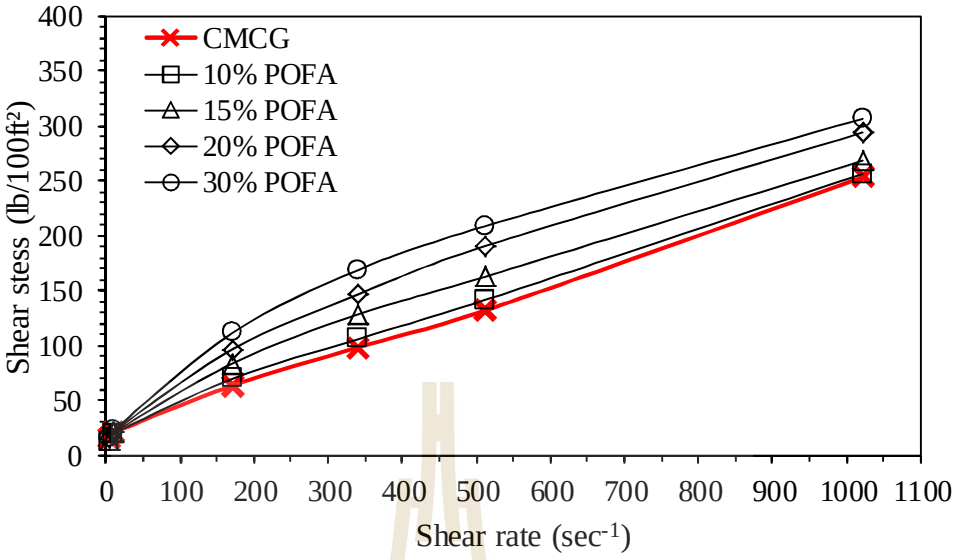

Figure 4.12 Consistency plot of POFA at room temperature

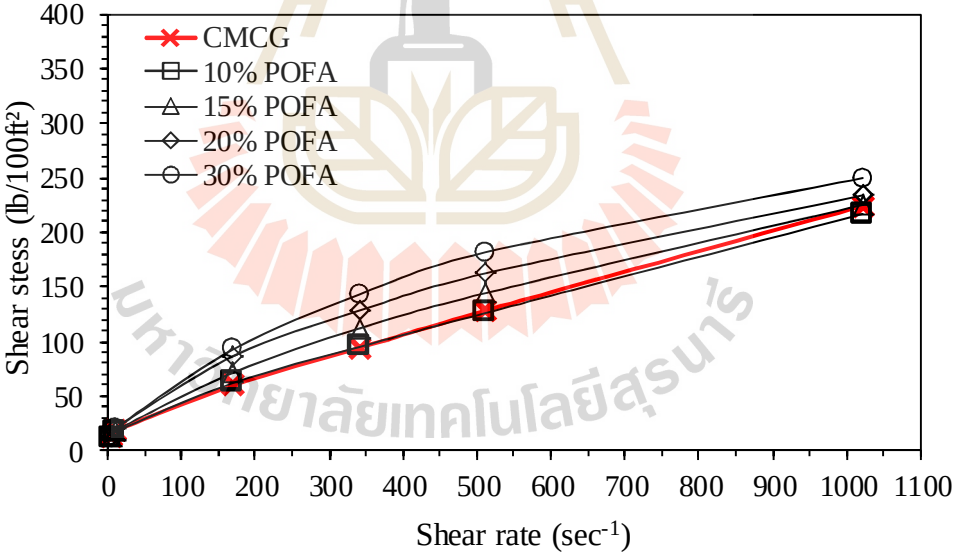

Figure 4.13 Consistency plot of POFA at 80˚C

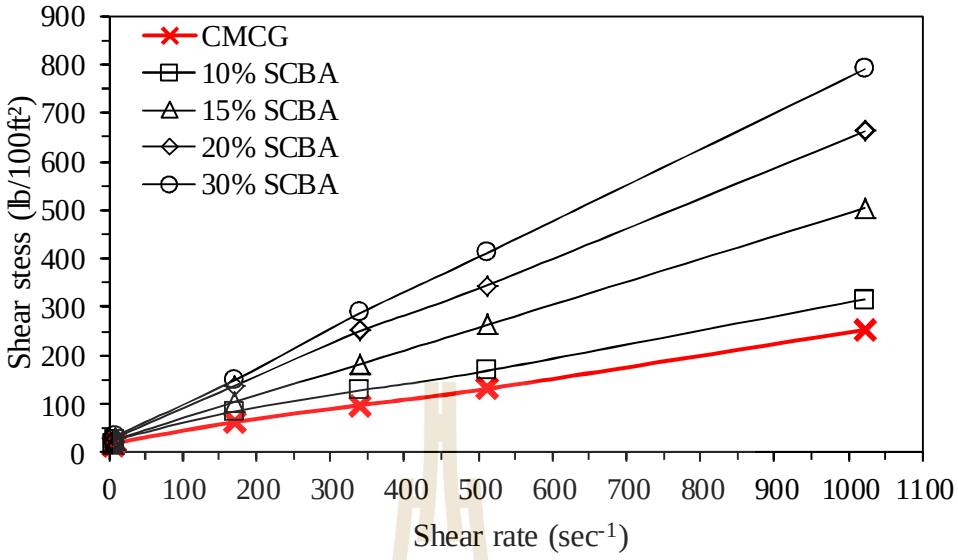

Figure 4.14 Consistency plot of SCBA at room temperature

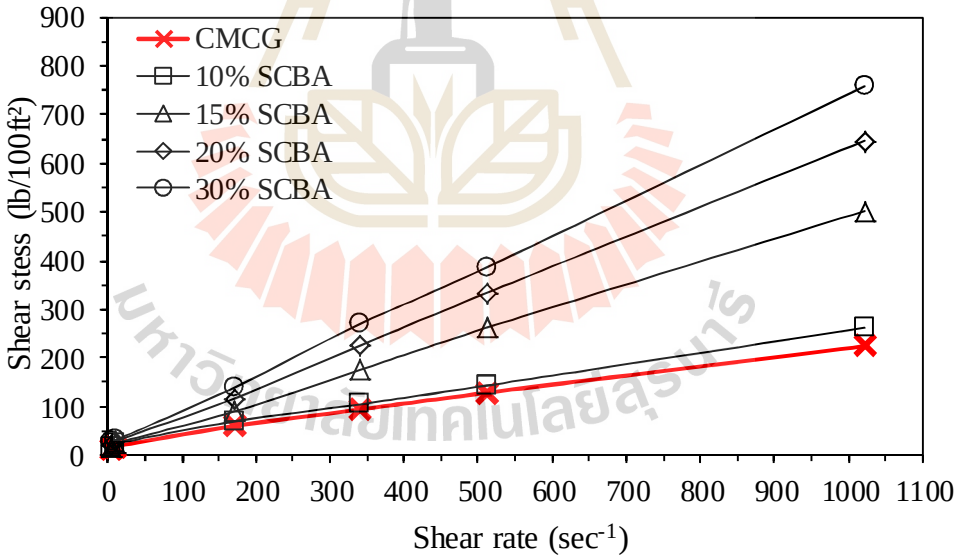

Figure 4.15 Consistency plot of SCBA at 80˚C

The Power's Law model parameters in the term of flow behavior index (n) and consistency (k) were calculated by equations (3.6) and (3.7) as showed in previous chapter. The index n indicated that all pozzolan cement slurry samples exhibited Pseudoplastic flow with n less than 1. As previous mentioned the flow behavior of typical oil well cement usually acted between the Bingham Plastic and the Power's Law model which was called Pseudoplastic fluid. The consistency factors of all pozzolanic cement slurry samples clearly increase with the increasing of the pozzolanic materials mixed ratio. The constant was analogous to the apparent viscosity of the fluid that described the thickness of the fluid. The Power's Law model did not describe the behavior of cement slurry exactly but the constant n and k normally desirable in the interest of hydraulic horsepower utilization which was used in hydraulic calculations.

Figure 4.10 to Figure 4.18 are the plots of the rheological parameters obtained from the calculation with various pozzolanic material mixed ratios. The apparent viscosity was plotted as a function of pozzolanic material mixed ratios as showed in Figure 4.16. Following Figure 4.16 it can be seen that apparent viscosity of SCBA and POFA cement slurry increases with the increasing of pozzolanic material mixed ratio, while the apparent viscosity of FLYA is slightly decreased both at room temperature and 80˚C condition.

When comparing apparent viscosity at between room temperature and 80˚C, it was found that apparent viscosity of SCBA and POFA cement slurry was decreased with increasing temperature. However, it was noticed that the apparent viscosity of FLYA cement slurry was slightly increased with increasing temperature. This is due to greater colloidal fraction of FLYA in cement slurry sample that result in

increasing of flow resistance. This is because the consequence of temperature increases interaction energy of mud and cement system (Luckham and Rossi, 1999). This interaction induces more inter-particle attractive force between solid particles and it brings the binder material particles come into contact with another and agglomerate which is known as flocculation.

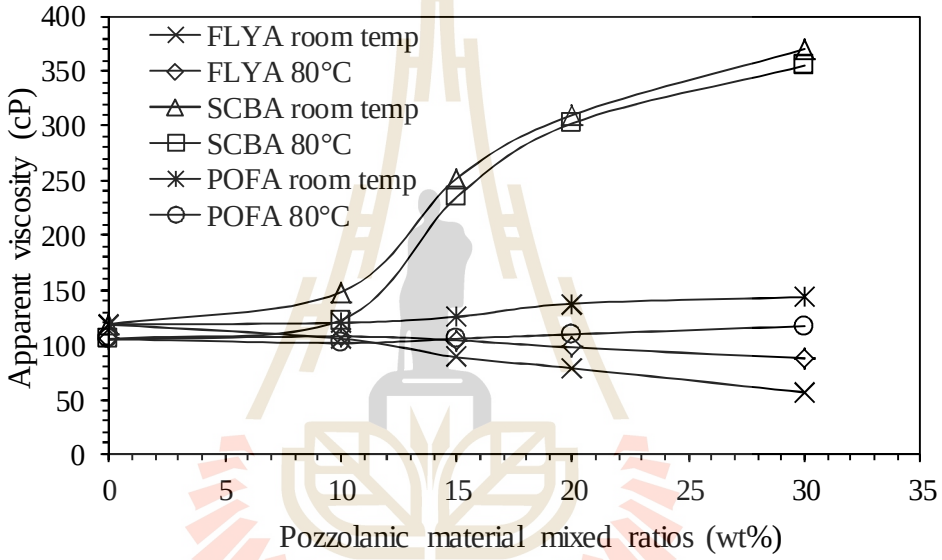

Figure 4.16 Apparent viscosity versus pozzolanic material mixed ratios

The Bingham plastic model in the term of plastic viscosity was also plotted versus pozzolanic material mixed ratios with both temperature conditions in this study as shown in Figure 4.17. Figure 4.17 indicates that plastic viscosity of SCBA and POFA cement slurry increases with the increasing of pozzolan material mixed ratio, while the plastic viscosity of FLYA cement slurry is slightly decreased both at room temperature and 80˚C likewise apparent viscosity. Considering effect of

elevated temperature, the influence of elevated temperature treatment slightly decreased of plastic viscosity after elevating temperature from room temperature to 80˚C. The trend of line indicated that the slurry cement behaved non-Newtonian and displayed lower plastic viscosities and higher yield stress. The effect of temperature on binder material suspension could be described as follows: heating up the binder material suspension increased the conductivity of the system. This was indicated that more cat-ions (Na^+) were dissolved from the surface of the particles. It was also suggested that this effect was responsible for the reduction of the normalized plastic viscosity and the observed of the yield stress increasing, the latter also due to thermal induced swelling (Luckham and Rossi, 1999). Like apparent viscosity, the increasing of plastic viscosity of FLYA cement slurry when elevating temperature is caused from fly ash particles flocculation.

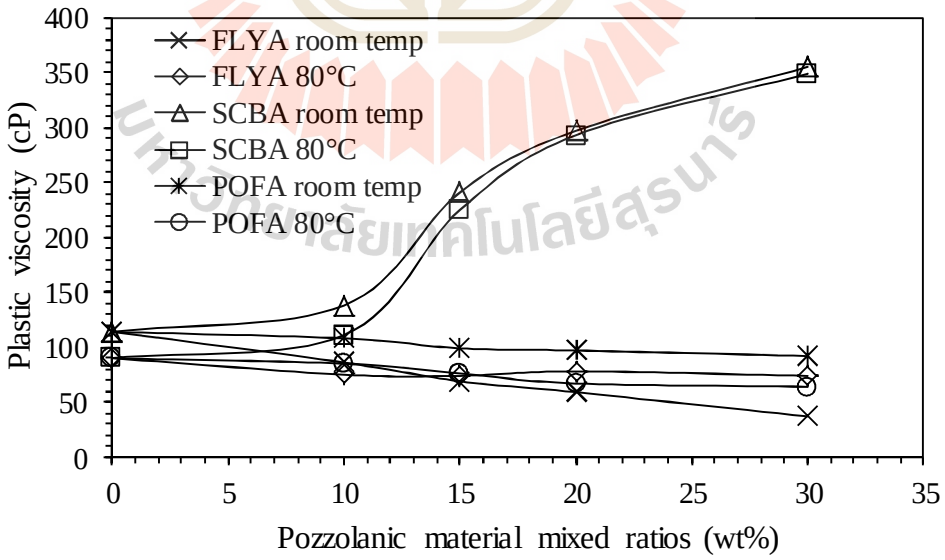

Figure 4.17 Plastic viscosity versus pozzolanic material mixed ratios

After plastic viscosity of each pozzolan cement slurry sample at various pozzolanic materials mixed ratios and at room temperature and 80˚C was calculated, yield point of each pozzolan cement slurry sample could be calculated by equation (3.3). Yield point from calculation was plotted versus pozzolanic material mixed ratios and showed in Figure 4.18. Figure 4.18 indicates that yield point of FLYA and SCBA slurry cement samples are slightly decreasing of pozzolanic material mixed ratios, while yield point of POFA cement slurry sample is dramatically increased. This is because large amount of palm oil fuel ash solid particle in cement slurry sample tend to agglomerate and result in increasing yield stress.

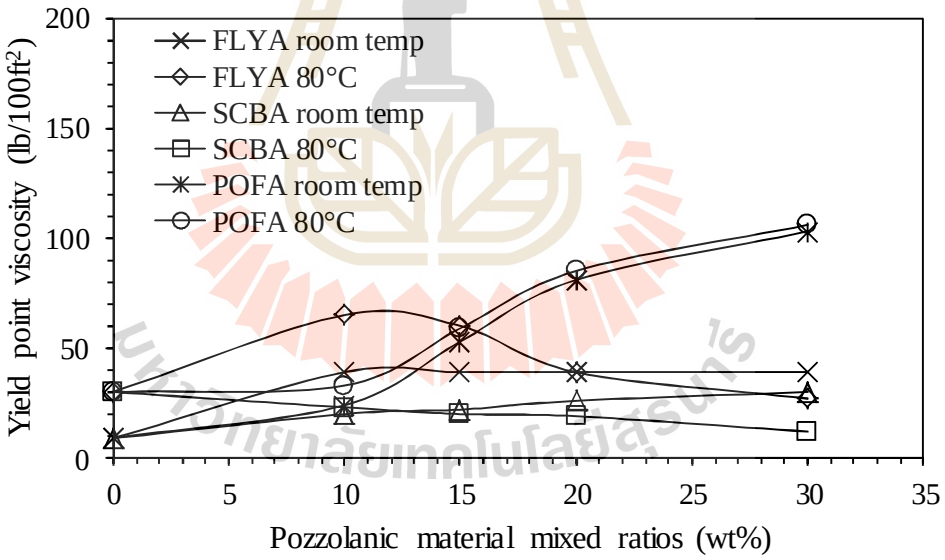

Figure 4.18 Yield point viscosity versus pozzolanic material mixed ratios

4.4.3 Fluid filtration

Cement slurry samples filtrate loss volume was measured by filtration test apparatus as showed in Figure 3.5. Results of measurements are shown in Figure 4.19 to Figure 4.21.

Results of filtrate volume measurement in this study indicated that the filtrate volume of all type pozzolan cement slurry samples was inverse proportional to the pozzolanic material amount. This may cause by the pozzolanic material is belter flocculated when having more pozzolanic materials content in pozzolan cement slurry. It was also noticeable that when the temperature was elevated, the amount of filtrate volume was also decreased. This may cause from water vaporization and result in more inter-particles attractive force between pozzolanic material particles and these particles can come into contact with another and agglomerate more easily.

Moreover, it can be observed from Figure 4.19 to Figure 4.21 that the fluid loss volume of among these pozzolan cement slurry in resending order are of POFA, SCBA, and FLYA cement slurry sample, respectively. Therefore, it can be concluded that in term of fluid loss prevention on application POFA is the most applicable among these three selected pozzolanic material and followed by SCBA and FLYA, respectively.

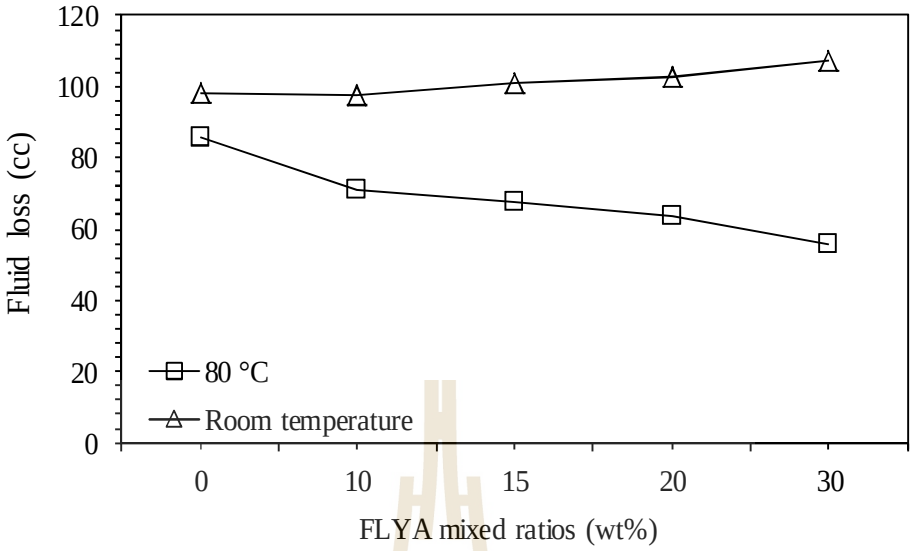

Figure 4.19 Fluid loss versus FLYA mixed ratios

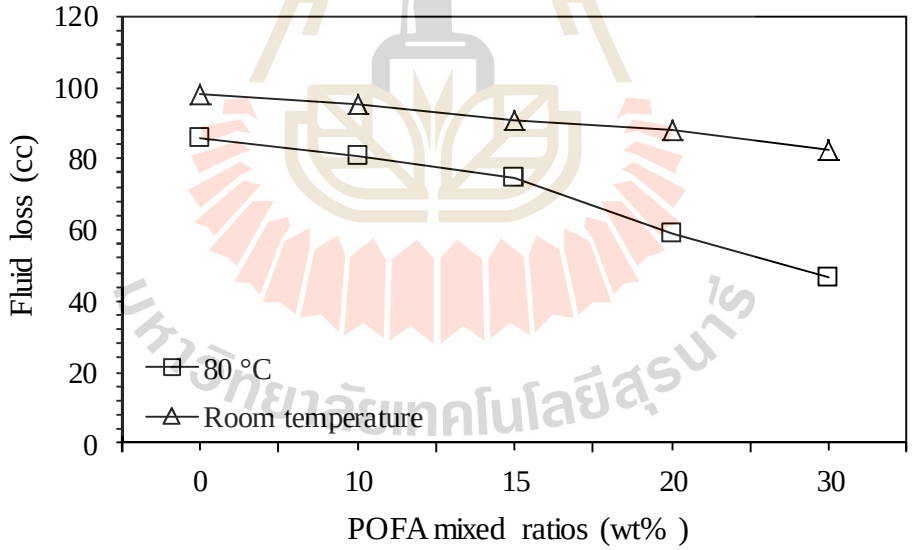

Figure 4.20 Fluid loss versus POFA mixed ratios

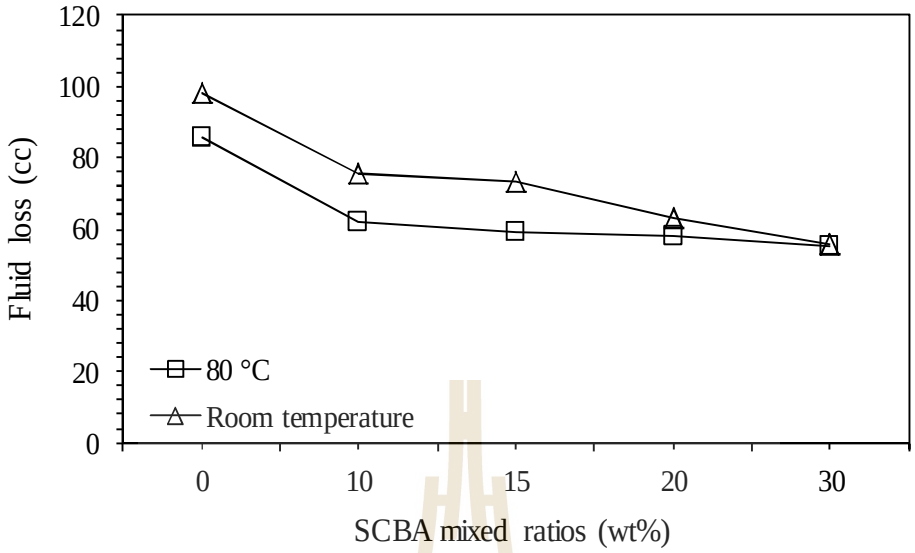

Figure 4.21 Fluid loss versus SCBA mixed ratios

4.4.4 Thickening time

Thickening (setting) times of set pozzolan cement at various mixed ratios were measured by the Vicat apparatus at the Civil Engineering Laboratory, Suranaree University of Technology. Results of the measurement are shown in Figure 4.22 to Figure 4.24 respectively.

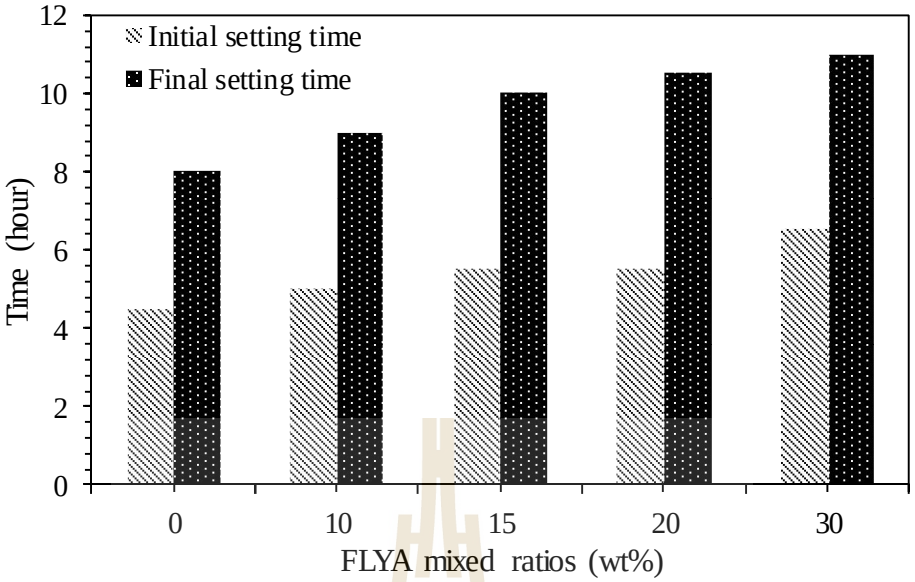

Figure 4.22 Initial and final setting time of FLYA cement

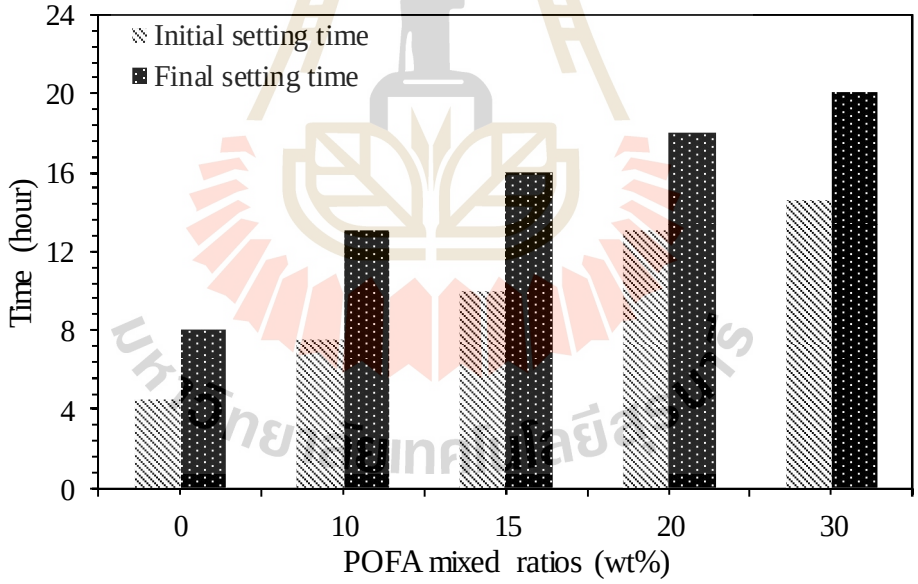

Figure 4.23 Initial and final setting time of POFA cement

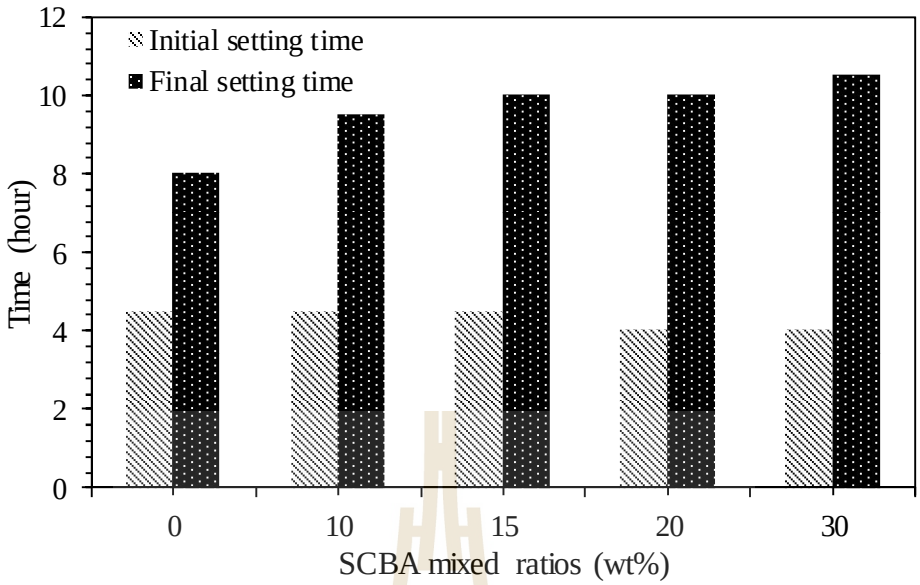

Figure 4.24 Initial and final setting time of SCBA cement

Results of the selected pozzolan cement indicated that most of the initial and final setting time of the pozzolan cement was directly proportional to the amount of pozzolanic material. The exception was only for the initial setting time of SCBA cement slurry. This may cause from the high water absorption ability of sugarcane bagasse ash particles and result in having its plasticity behavior longer than others.

4.5 Set pozzolan cement sample properties

4.5.1 Compressive strength

The results of compressive strength measurement of set pozzolan cement samples showed that the compressive strength of all selected pozzolanic materials tended to improve when the pozzolanic material to cement mixed ratio was

increased at room temperature as depicted in Figures 4.25, 4.27, and 4.29.

However, it was found that the compressive strength of all selected pozzolanic material was reduced when the mixed ratio was higher than 20 wt%. The most problem of the pozzolanic material used for cementitious material mixed in cement are limited with the quantities of calcium hydroxide ($Ca(OH)_2$). An increasing pozzolanic material mixed ratio will decrease an amount of cement, that impact directly on the quantity of $Ca(OH)_2$ for the pozzolanic reaction. In the addition, that the compressive strength of FLYA was slightly higher than SCBA and POFA concrete for the same mixed ratio, respectively. Since the total amount of SiO_2, Al_2O_3, Fe_2O_3 and CaO of each selected pozzolanic material effect directly to the strength of concrete.

Figures 4.26, 4.28, and 4.30 depict the experimental results of concrete samples at 80˚C condition. The results also presented the relationship in the similar direction as the experimental results of concrete samples at room temperature.

However, the experiments results indicated that the compressive strength of concrete sample with 50 days concrete curing is much lower than concrete sample with 7 and 28 days concrete curing for 80˚C condition, respectively. Since the high temperature can accelerate the hydration reaction (Sukontasukkul, 2006), but the byproducts of hydration reaction are not well consolidated throughout the entire concrete, this results impact decreasing on compressive strength of concrete (Kosmatka et al., 2003).

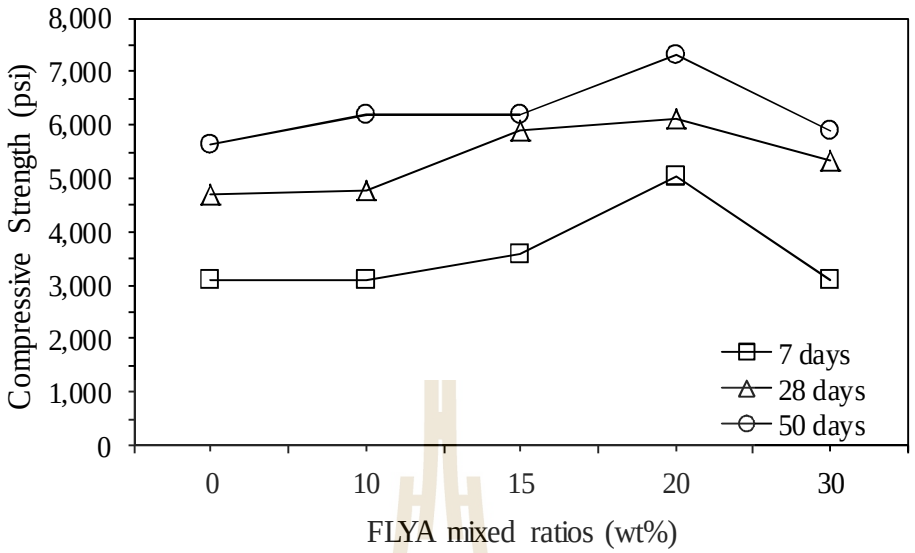

Figure 4.25 Compressive strength versus FLYA mixed ratios at room temperature

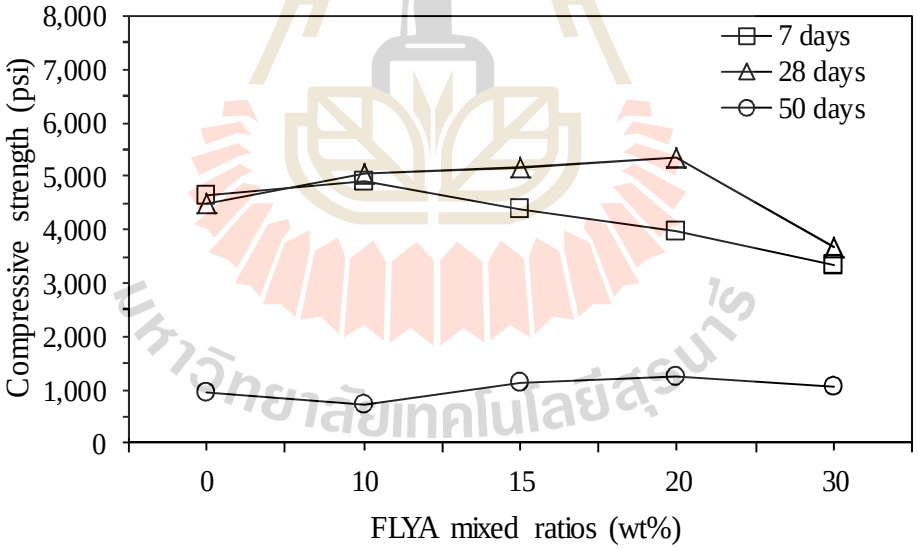

Figure 4.26 Compressive strength versus FLYA mixed ratios at 80˚C

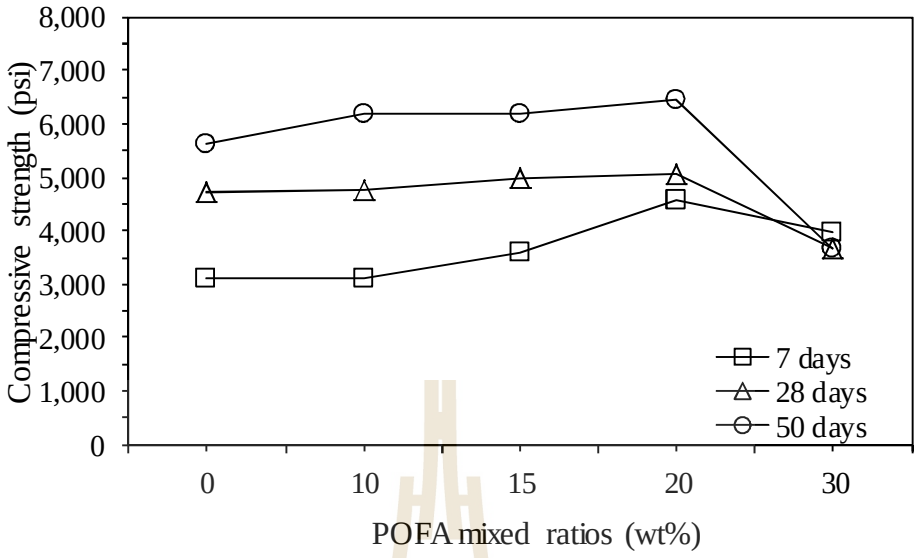

Figure 4.27 Compressive strength versus POFA mixed ratios at room temperature

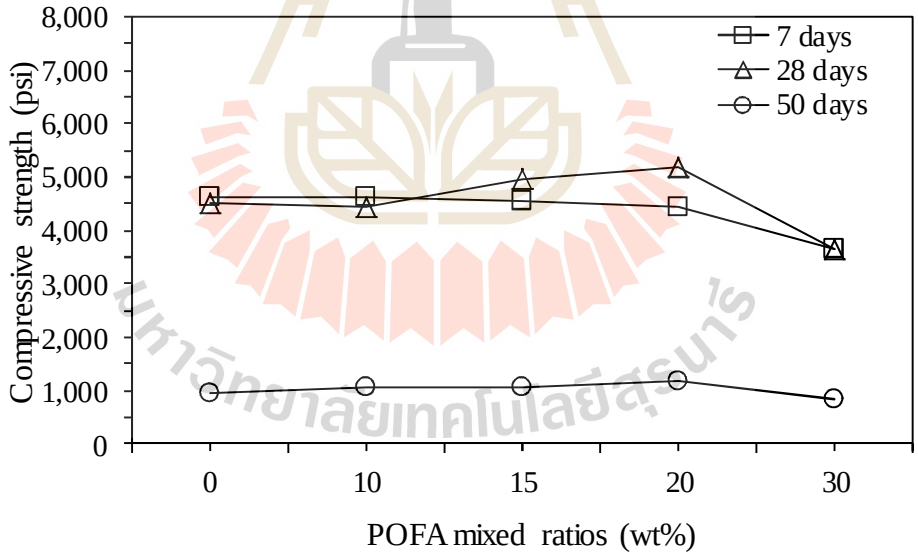

Figure 4.28 Compressive strength versus POFA mixed ratios at 80˚C

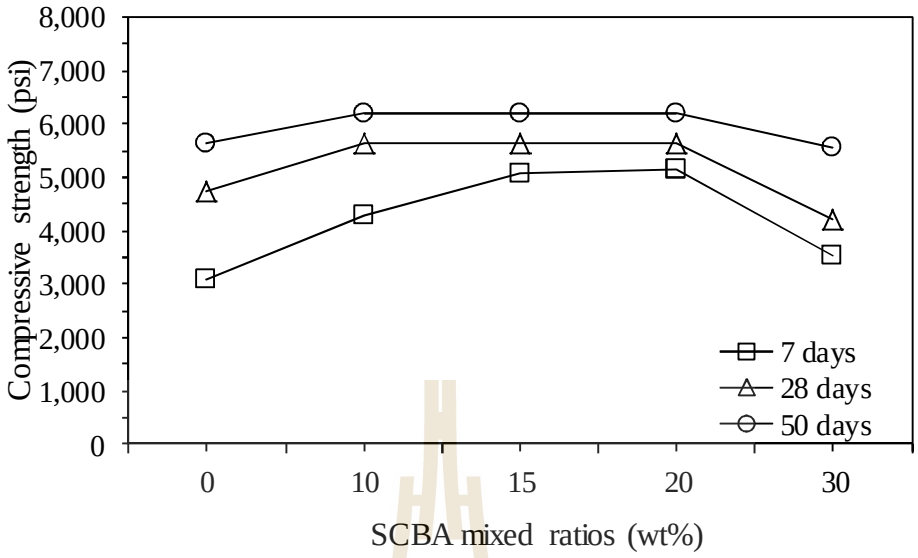

Figure 4.29 Compressive strength versus SCBA mixed ratios at room temperature

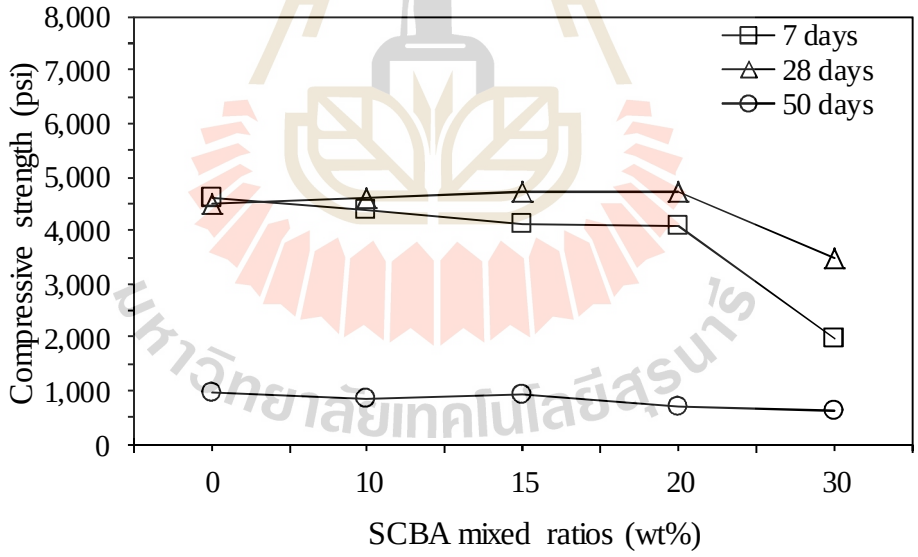

Figure 4.30 Compressive strength versus SCBA mixed ratios at 80˚C

4.5.2 Permeability

The set pozzolan cement specimen of each selected mixing pozzolanic material at curing time of 7, 28, and 50 days was measured its permeability by using Permeameter apparatus at the Geotechnology Laboratory, Suranaree University of Technology. Each set pozzolan cement specimen was measured its permeability at various pressure level. In this study the overburden pressure (BP) were set at 200 psi (for low pressure test) and 2000 psi (for high pressure test), while the formation pressure (P_1) was fixed at 20 psi. Results of permeability measurement are showed in Figure 4.31 to Figure 4.34, respectively.

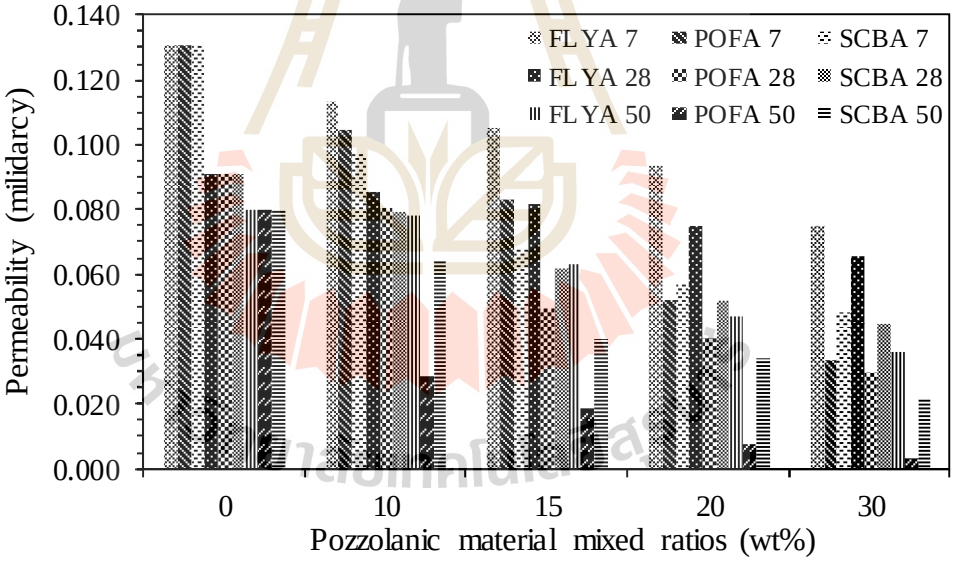

Figure 4.31 Permeability versus pozzolanic material mixed ratios at room temperature and BP=200 psi

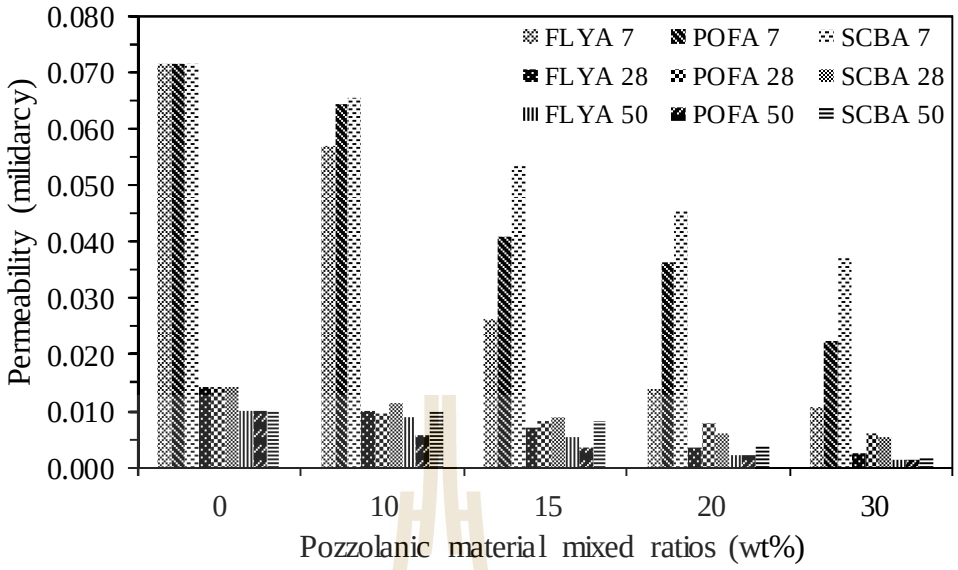

Figure 4.32 Permeability versus pozzolanic material mixed ratios at 80˚C and BP=200 psi

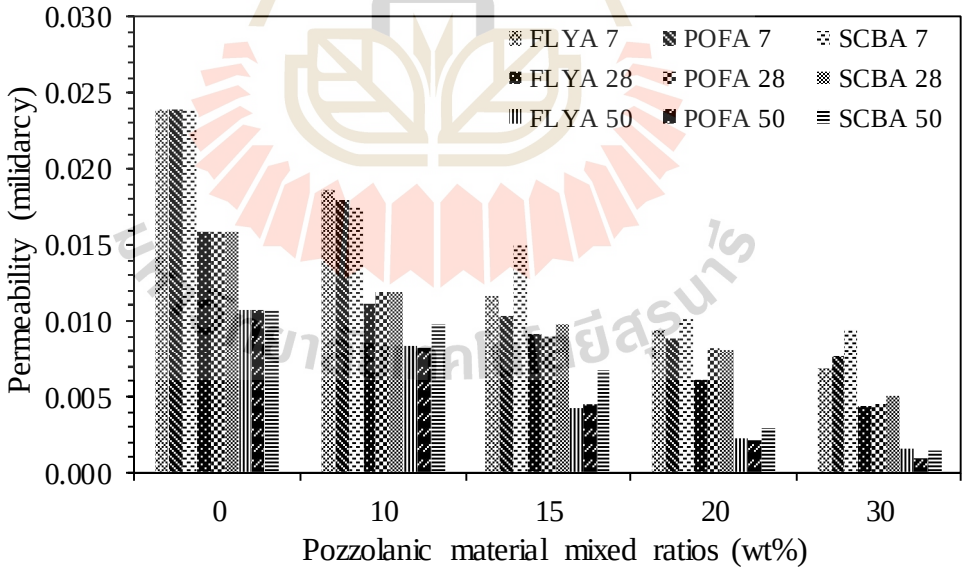

Figure 4.33 Permeability versus pozzolanic material mixed ratios at room temperature and BP=2000 psi

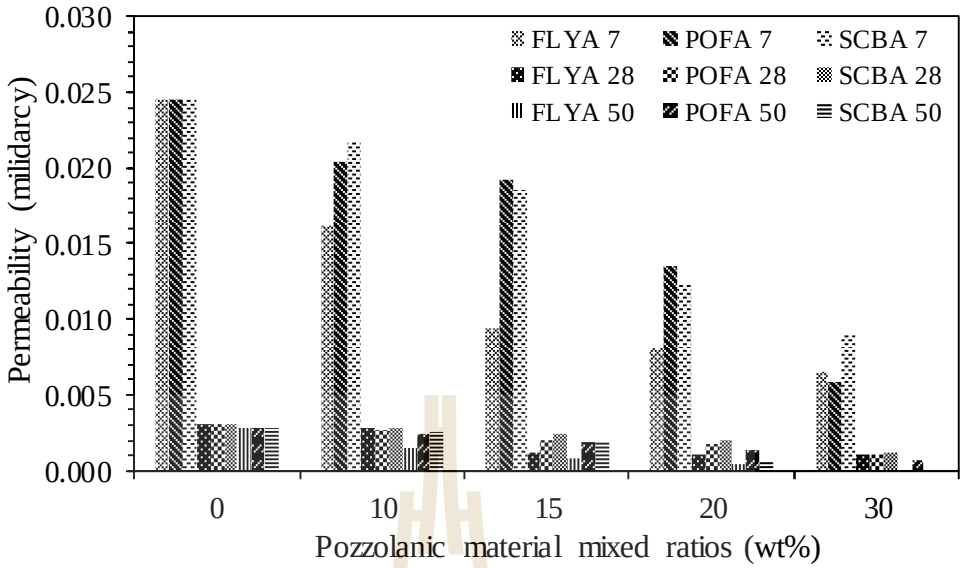

Figure 4.34 Permeability versus pozzolanic material mixed ratios at 80˚C and BP=2000 psi

Follow Figure 4.31 to Figure 4.34, it was found that the permeability was reversely proportional to the weight percentages of pozzolanic material. The permeability was decreased when the weight percentage of pozzolanic material was increased. This is because pozzolanic material used in this study contained very high quartz (SiO_2) content. According to the pozzolan reaction, quartz (SiO_2) will react with calcium hydroxide ($Ca(OH)_2$) and aluminium oxide (Al_2O_3) and product solid compound of calcium silicate hydrate (C-S-H) and calcium aluminate hydrate (C-A-H) as by- product. These crystals were fulfill the pore space of set pozzolan cement sample and further resulted in decreasing of the amount of pore space and permeability.

Moreover, it was also found that permeability of the set pozzolan cement sample was reversely proportional to the tested overburden pressure. This is because when the overburden pressure is increased, the cement compaction is also increased and resulted in decreasing of permeability.

4.6 Relationship among density, permeability and compressive strength of set pozzolan cement samples

4.6.1 Density and compressive strength

Since the compressive strength of set pozzolan cement sample curing at 28 days was higher than these of 7 and 50 days curing time. Therefore, density and compressive strength values of FLYA, POFA and SCBA cement slurry of sample with 28 days concrete curing at room temperature and at 80°C were plotted to determine the optimum selected pozzolanic material to cement mixed ratio. Results of the plots are showed in Figure 4.35 and Figure 4.36. In the addition, it can be observed that the pozzolanic material to cement mixed ratio of both temperature at 20 wt% for all material has the highest compressive strength compared to 10, 15 and 30 wt%. Therefore, the proper FLYA, POFA and SCBA to cement mixed ratio should be range between 15 and 20 wt% following experimental results.

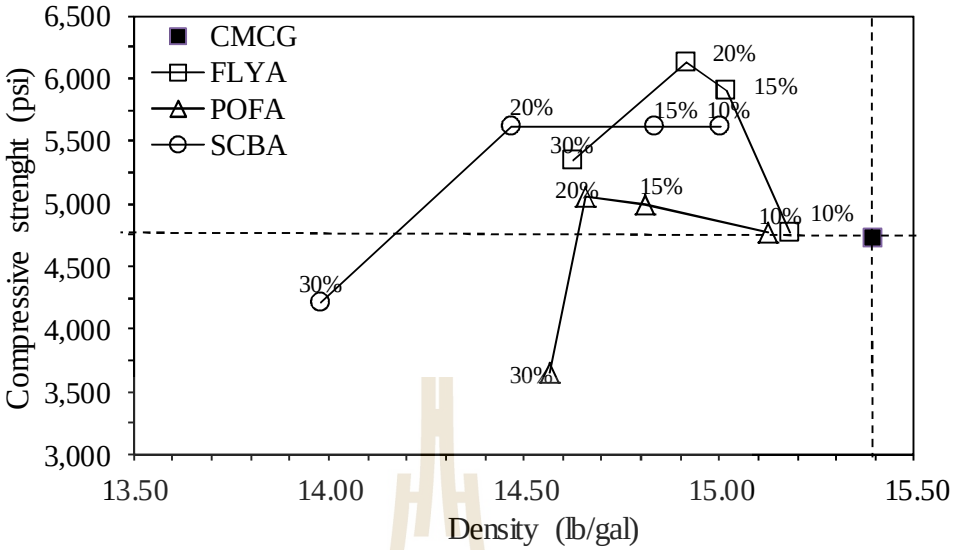

Figure 4.35 Density and compressive strength at room temperature

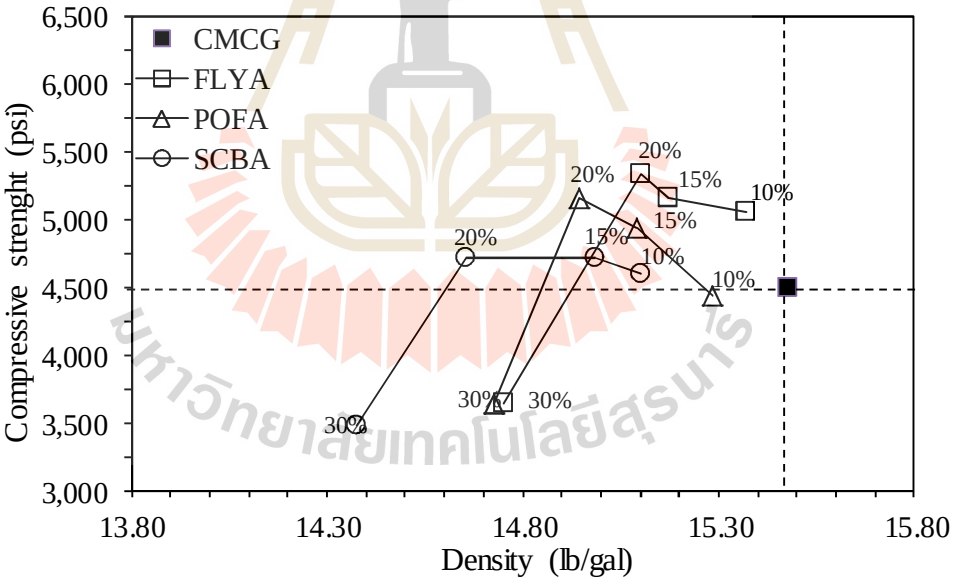

Figure 4.36 Density and compressive strength at 80˚C

4.6.2 Permeability and compressive strength

Permeability measured at overburden pressure of 200 psi and 2000 psi and compressive strength values of FLYA, POFA and SCBA set cement sample of 28 days curing time both at room temperature and 80˚C were plotted and observed to determine the optimum selected pozzolanic material to cement mixed ratio. Results of the plots are presented in Figure 4.37 to Figure 4.40.

It can be observed from all of the plots that the pozzolanic material mixed ratio at 20 wt% of every set pozzolan cement samples gave the highest compressive strength value and followed by 15, 10, and 30 wt%, respectively. It was also found that at this mixed ratio the permeability of set pozzolan cement sample was low. Therefore, the recommended mixing ratio of FLYA, POFA, and SCBA to use as an additive of API class G cement should be range between 15 to 20 wt%.

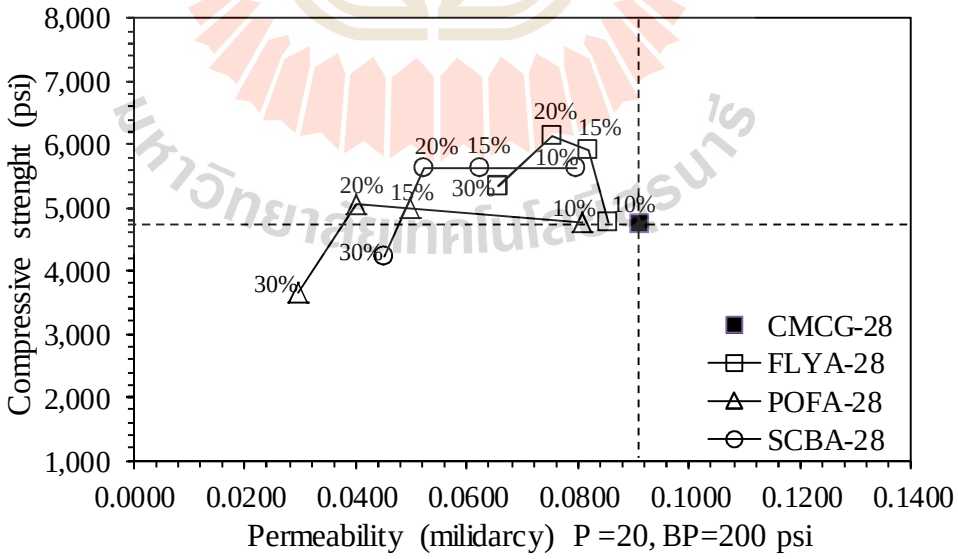

Figure 4.37 Permeability and compressive strength at room temperature, 200 psi

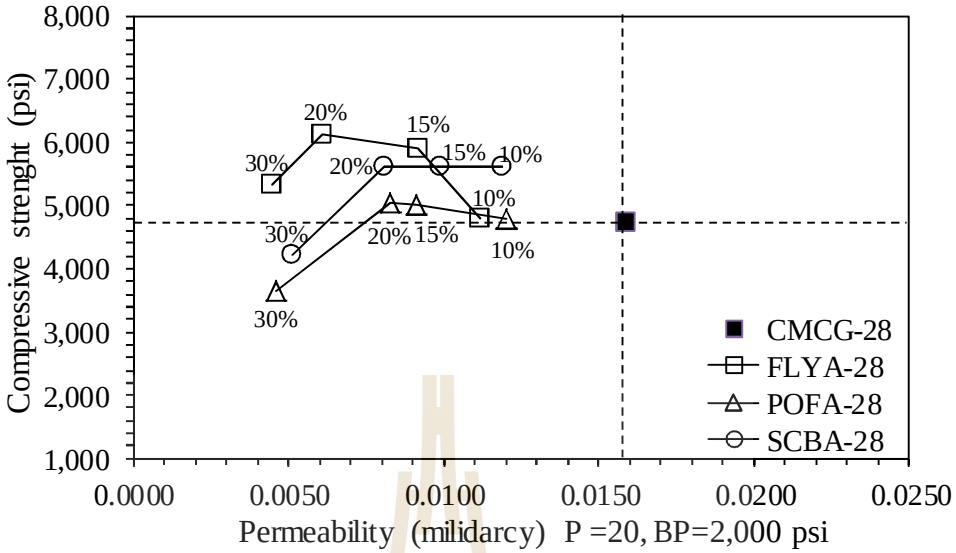

Figure 4.38 Permeability and compressive strength at room temperature, 2,000 psi

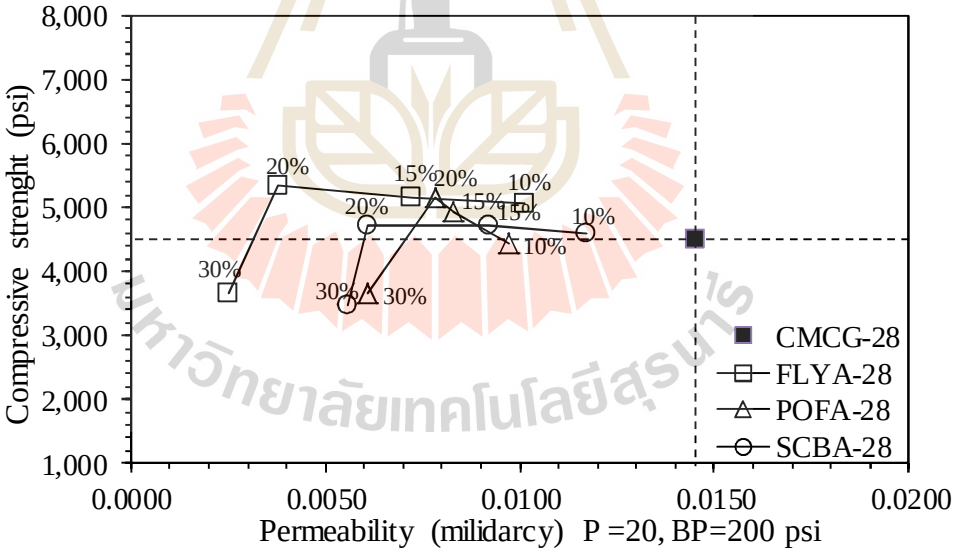

Figure 4.39 Permeability and compressive strength at 80˚C, 200 psi

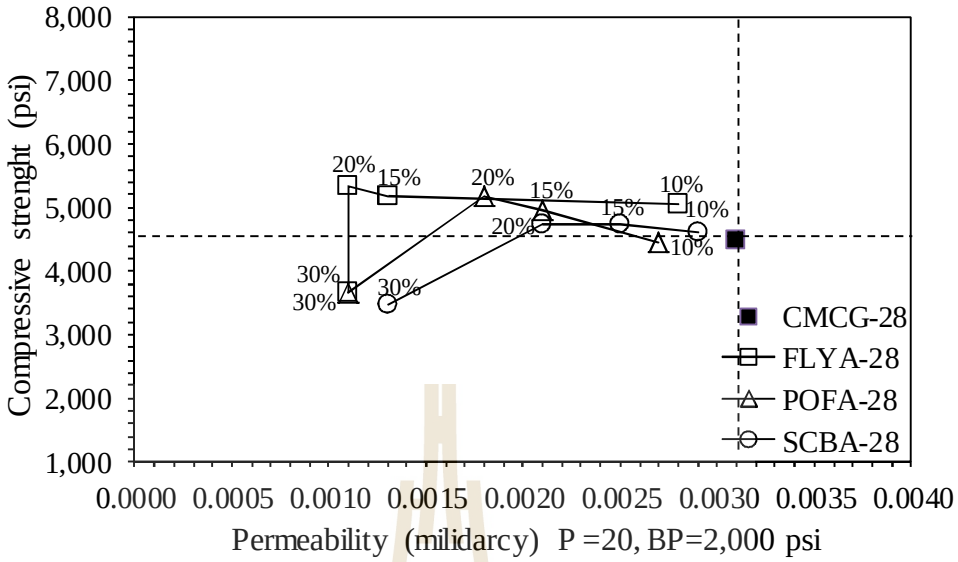

Figure 4.40 Permeability and compressive strength at 80˚C, 2,000 psi

CHAPTER V

CONCLUSIONS AND RECOMMENDATIONS

5.1 Conclusions

Based on the experiments and measurements of this study, pozzolanic material chemical compound, physical properties, including density, viscosity and filtrate volume, thickening time, compressive strength, and permeability of cement mixed with FLYA, POFA, SCBA, and API class G cement concluded and summarized as follows.

5.1.1 Chemical compound

Results from XRF analysis indicated that the selected pozzolanic material sample used in this study was consisted mainly of SiO_2 +Al_2O_3 + Fe_2O_3 as prescribed by ASTM C 618. The result also revealed that the SCBA and the FLYA can be classified as class F and class C pozzolan as prescribed by ASTM C 618, respectively. The POFA cannot be classified as pozzolan because the contents of SiO_2 +Al_2O_3 + Fe_2O_3 were less than 50%.

5.1.2 Physical properties

All of the selected pozzolanic material had specific gravity lower than CMCG and the specific gravity of SCBA was the lowest in this experiment. After sieving until the size of the selected pozzolan materials is less than 45 µm, it was found that the particle shape of FLYA was spherical. The particle surface was smooth which indicated a rather complete burning. The particle shape of POFA was rather

spherical and they had irregular surface which was similar to those of CMCG. However, POFA had less porosity in particle surface than CMCG. SCBA had various particle shapes more than other selected pozzolan, including shape tabulate and fibrous. This SCBA particle also had porous more than others. The water-to binder (W/B) ratios of SCBA concretes were higher also than other pozzolanic concrete and result in the higher replacement ratios.

5.1.3 Pozzolan cement slurry test

It was found from the study that density of pozzolan cement was directly proportional to the amount of pozzolanic materials. Therefore, the selected pozzolanic materials in this study can be used as an extender additive for the oil well cement. However, the density of the selected pozzolan cement slurry was increased when the test temperature was elevated from room temperature to 80°C due to the water loss during temperature elevating.

Moreover, the larger amount of selected pozzolanic materials can cause the cement slurry more viscous because the hydration and pozzolanic reaction can be taken place more easily and quickly.

Fluid loss volume measurement on pozzolan cement slurry indicated that in the plastic phase fluid loss volume of pozzolan cement slurry was reversely proportional to the amount of pozzolanic materials both at room temperature and at 80˚C.

The thickening time measurement revealed that both of the initial and the final thickening time of cement slurry was directly proportional to the increasing pozzolanic weight percent replacement. This is except only for the initial time of SCBA slurry cement because the SCBA particles have more pores than other selected

pozzolanic materials. From this thickening time measurement, it was found that POFA can prolong the thickening time more than other selected pozzolanic materials. Therefore, POFA can be used as a retarder additive for oil well cement as well.

5.1.4 Set pozzolan cement test

Compressive Strength

Results from compressive strength measurement indicated that the compressive strength of set cement was directly proportional to the amount of pozzolanic material mixed ratios. This is because the pore space within set cement specimen is replaced by calcium silicate hydrate (C-S-H) and calcium aluminates hydrate (C-A-H) and resulted in pore space decreasing. Since pozzolanic material samples used in this study is composed of very high SiO_2 content, this may cause enough silicon dioxide that would react with calcium hydroxide fluid in pore space and then resulted in compressive strength enhancing.

Permeability

This study also found that the permeability of set cement specimens was reversely proportional to the amount of pozzolanic material weight percent. The reason might be the same as in the compressive strength enhancing that silicon dioxide reacted to calcium hydroxide liquid in concrete pore space. The by-product as solid calcium silicate hydrate crystals were filled up the pore space of the set cement specimens and made these pores smaller.

It can be concluded that the selected pozzolanic materials can be used as an oil well API class G cement additive if it is used to replace oil well API class G cement at range between 15-20 wt%. This is because with this replacement ratio the filtrate loss

volume and viscosity of the cement slurry are not much different from those of the cement without pozzolanic material while the density is lowered. Moreover, these selected pozzolanic materials can increase the compressive strength and can also reduce the permeability of the set cement specimens effectively.

5.2 Recommendations

For the future study, pozzolanic materials samples should be collected from various places to study the effect of SiO_2 content and the physical properties and rheological properties of set cement and cement slurry.

Tested temperature should be elevated to higher than 80°C to study the effect of temperature to the pozzolanic effect since the real bottom hole temperature of petroleum well is normally higher than 80°C. Other inexpensive, abundant and/or agricultural wastes, e.g. rice straw and saw dust, should be tested their pozzolanic properties to use it as an oil well cement additive.

REFERENCES

, , . (2548). (Cement and Applications). (4). : .

Abbasi, A. and Zargar, A. (2013). Using bagasse ash in concrete as pozzolan. Middle-East Journal of Scientific Research. 13(6): 716-719.

Abdullah, K., Hussin, M. W., Zakaria, F., Muhamad, R., and Hamid, A.Z. (2006). POFA: A potential partial cement replacement material in aerated concrete. In Proceedings of the 6th Asia-Pacific Structural Engineering and Construction Conference (pp 1-5). Kuala Lumpur, Malaysia.

Ahmaruzzaman, M. (2010). A review on the utilization of fly ash. Progress in Energy and Combustion Science. 36(3): 327-363.

ASTM C 618. (2001). Standard specification for coal fly ash and raw or calcined natural pozzolan for use as a mineral admixture in concrete. Annual Book of ASTM Standard. 4(2): 310-313

Awal, A.S.M.A. and Hussin, M.W. (1997). The effectiveness of palm oil fuel ash in preventing expansion due to alkali-silica reaction. Cement and Concrete Composites. 19(4): 367-372

Awal, A.S.M.A. and Hussin, M.W. (1999). Durability of high performance concrete containing palm oil fuel ash. In Proceedings of the 8th International Conference on Durability of Building Materials and Components (pp 465-474). Vancouver, British Columbia, Canada.

Chindaprasirt, P., Homwuttiwong, S., Jaturapitakkul, C. (2007). Strength and water permeability of concrete containing palm oil fuel ash and rice husk–bark ash. Construction and Building Materials, (21):1492–1499.

Chindaprasirt, P., Rukzon, S., and Sirivivatnanon, V. (2008). Resistance to chloride penetration of blended portland cement mortar containing palm oil fuel ash, rice husk ash and fly ash. Construction and Building Materials. 22(5): 932-938.

Chusilp, N., Jaturapitakkul, C., and Kiattikomol, K. (2009). Utilization of bagasse ash as a pozzolanic material in concrete. Construction and Building Materials. 23: 3352–3358.

Cordeiro, G.C., Filho, T.R.D., Fairbairn, E.M.R., Tavares, L.M.M., and Oliveira, C.H. (2004). Influence of mechanical grinding on the pozzolanic activity of residual sugarcane bagasse ash. In Proceedings of the International RILEM Conference on the Use of Recycled Materials in Building and Structure (pp 731-740). Barcelona, Spain.

Halliburton, All Rights Reserved. (2003). Micro fly ash cement [On-line]. Available: http://www.halliburton.com/en-US/ps/cementing/materials-chemicals-additives /cement-blends/micro-fly-ash-cement.page?node-id=hfqelabn

Herianto, A., Fathaddin, M.T. (2005). Effects of additives and condi-tioning time on comprehensive and shear bond strengths of geothermal well cement. In Proceedings of World Geothermal Congress (pp 1–7). Antalya, Turkey.

Hussin, M.W., and Awal, A.S.M.A. (1996). Influence of palm oil fuel ash on strength and durability of concrete. In Proceedings of the 7th International Conference on the Durability of Building Materials and Components (pp 291-298). Stockholm, London, UK.

Isaia, G.C., Gastaldini, A.L.G and Moraes, R. (2003). Phasical and pozzolanic action of mineral addition on the mechanical strength of hogh performance concrete, Cement and concrete composition. 25: 69-76.

Kiattikomol, K., Jaturapitakkul, C., Songpiriyakij, S., and Chutubtim, S. (2001). A study of ground coarse fly ashes with different fineness from various sources of pozzolanic materials. Cement and Concrete Composites. 23(4-5): 335-343.

King, G. E. (2006). Chapter on Casing Design and Cementing in "Drilling Engineering" [On-line].Available: http://www.gekengineering.com/Down - loads/Free_Downloads/Cementing_Chapter_3.pdf

Kosmatka, S.H., Panarese, W.C., and Kerkhoff, B., (2003). Design and Control of Concrete Mixtures. 14th ed. Portland Cement Association, Skokie, IL, USA, 358p.

Kroehong, W., Sinsiri, T., Jaturapitakkul, C. and Chindaprasirt, P. (2012). A study microstructure of blended cement paste containing palm oil fuel ash, KMUTT Research and Development Journal. 35(2): 187-200.

Luckham, P.V. and Rossi, S., (1999). The colloidal and rheological properties of bentonite suspensions. J. Colloid Interface Sci. 82: 43-92.

Madurwar, M.V., Mandavgane, S.A. and Ralegaonkar, R.V. (2014). Use of sugarcane bagasse ash as brick material. Current Science. 107(6): 1044-1051.

Mitchell, R.F. (2006). Petroleum Engineering Handbook. Volume II: Drilling Engineering. Society of Petroleum Engineers, Richardson, TX, USA, 763p.

Modani P.O. and Vyavhare, M.R. (2013). Utilization of bagasse ash as a partial replacement of fine aggregate in concrete. Procedia Engineering (51): 25-29.

Paya, J., Monzo, J., Borrachero, M.V., Mora, E.P., and Lopez, E. G. (1996). Mechanical treatment of fly ashes part II: particles morphology in ground fly ashes (GFA) and workability of GFA-cement mortars. Cement and Concrete Research. 26(2): 225-235.

Safiuddin, M., Salam, M.A., and Jumaat, M.Z. (2011). Utilization of palm oil fuel ash in concrete: a review. Journal of Civil Engineering and Management. 17(2): 234-247.

Sata, V., Jaturapitakkul, C., and Kiattikomol, K. (2004). Utilization of palm oil fuel ash in high-strength concrete. Journal of Materials in Civil Engineering. 16(6): 623-628.

Sata, V., Jaturapitakkul, C., and Kiattikomol, K. (2007). Influence of pozzolan from various by-product materials on mechanical properties of high-strength concrete. Construction and Building Materials. 21(7): 1589-1598.

Schettino, M.A.S., and Holanda, J.N.F. (2015). Processing of porcelain stoneware tile using sugarcane bagasse ash waste. In Processing and Application of Ceramics. 9(1): 17-22.

Serametjakun, P., (2001). Utilization of Limestone Powder with Pozzolanic Material. M.S. thesis, Thammasat University, Thailand

Sivakumar, A.D.V.S., Balaji, K.V.G.D. and Santhoshkumar, T. (2014). Behavior of sugarcane bagasse ash concrete exposed to elevated temperature. International Journal of Advance Research in Science and Engineering. 3(7): 355-359.

Society of Petroleum Engineers. (2015). Cementing operations [On-line]. Available: http://petrowiki.org/Cementing_operations

Somna, R. and Jaturapitakkul, C. (2011). Use of ground bagasse ash to improve compressive strength, water permeability and chloride resistance of recycled aggregate concrete. KMUTT Research and Development Journal. 34(4): 369-381.

Srinivasan, R. and Sathiya, K. (2010). Experimental Study on Bagasse Ash in Concrete. International Journal for Service Learning in Engineering. 5(2): 60-66.

Sukantapree, S., Namarak, C., and Jaturapitakkul, C. (2002). Use of calcium carbide residue and palm oil fuel ash in concrete. In Proceedings Annual Conference of the Engineering Institute of Thailand (pp 191-199). Bangkok, Thailand.

Sukontasukkul, P. (2006). Concrete fundamentals. King Mongkut's University of Technology North Bangkok, Bangkok, Thailand, 179p.

Sumadi, S. R., and Hussin, M. W. (1995). Palm oil fuel ash (POFA) as a future partial cement replacement material in housing construction. Journal of Ferrocement. 25(1): 25-34.

Tangchirapat, W., Jaturapitakkul, C., and Chindaprasirt, P. (2009). Use of palm oil fuel ash as supplementary cementitious material for producing high-strength concrete. Construction and Building Materials. 23(7): 2641-2646.

Tangchirapat, W., Saeting, T., Jaturapitakkul, C., Kiattikomol, K., and Siripanichgom, A. (2007). Use of waste ash from palm oil industry in concrete. Waste Management. 27(1): 81-88.

Tangchirapat, W., Tangpakasit, J., Waew-kum, S. and Jaturapitakkul, C. (2003). A new pozzolanic material from palm oil fuel ash, KMUTT Research and Development Journal. 26(4): 459-473.

Tay, J. H. (1990). Ash from oil-palm waste as concrete material. Journal of Materials in Civil Engineering. 2(2): 94-105.

Thomas O. A. and Alan P. R. (2006). Production Operations: Well Completions, Workover and stimulations (Vols. 1) (5th ed.). Oklahoma: OGCI and PretroSkills Publications.

Tijore, N.A., Pathak, V.B. and Shah, R.A. (2013). Utilization of sugarcane bagasse ash in concrete. International Journal for Scientific Research & Development. 1(9): 1938-1942.

Tonnayopas, D., Nilrat, F., Putto, K., and Tantiwitayawanich, J. (2006). Effect of oil palm fiber fuel ash on compressive strength of hardening concrete. In Proceedings of the 4th Thailand Materials Science and Technology Conference (pp 1–3). Pathumthani, Thailand.

APPENDIX A

EXPERAMENTAL DATA

Pressurized Fluid Balance results data

Table A.1 Density for Pozzolanic material

Mixed wt%	FLYA (lb/gal)		POFA (lb/gal)		SCBA (lb/gal)	
	Room temperature	80°C	Room temperature	80°C	Room temperature	80°C
0%	15.39	15.47	15.39	15.47	15.39	15.47
10%	15.17	15.37	15.12	15.28	15.00	15.10
15%	15.06	15.25	14.81	15.09	14.83	14.98
20%	14.91	15.10	14.65	14.94	14.47	14.65
30%	14.62	14.74	14.56	14.72	13.97	14.37

Fan viscometer results data

Table A.2 Viscosity for mixed ratios with FLYA

Mixed wt%	Room temperature			80°C		
	μ_p (cp)	μ_a (cp)	γ_p (lb/100 ft^2)	μ_p (cp)	μ_a (cp)	γ_p (lb/100 ft^2)
FLYA 0%	114.0	118.5	9.0	90.0	105.0	30.0
FLYA 10%	86.0	105.5	39.0	75.0	107.5	65.0
FLYA 15%	69.0	88.5	39.0	74.0	104.0	60.0
FLYA 20%	59.0	78.5	39.0	78.0	97.5	39.0
FLYA 30%	37.0	56.5	39.0	74.0	87.5	27.0

Table A.3 Viscosity for mixed ratios with POFA

Mixed wt%	Room temperature			80°C		
	μ_p (cp)	μ_a (cp)	γ_p (lb/100 ft^2)	μ_p (cp)	μ_a (cp)	γ_p (lb/100 ft^2)
POFA 0%	114.0	118.5	9.0	90.0	105.0	30.0
POFA 10%	108.0	120.0	24.0	85.0	101.5	33.0
POFA 15%	99.0	125.5	53.0	76.0	105.5	59.0
POFA 20%	97.0	137.5	81.0	67.0	109.5	85.0
POFA 30%	92.0	143.5	103.0	64.0	117.0	106.0

Table A.4 Viscosity for mixed ratios with SCBA

Mixed wt%	Room temperature			80°C		
	μ_p (cp)	μ_a (cp)	γ_p (lb/100 ft^2)	μ_p (cp)	μ_a (cp)	γ_p (lb/100 ft^2)
SCBA 0%	114.0	118.5	9.0	90.0	105.0	30.0
SCBA 10%	138.0	148.0	20.0	111.0	122.5	23.0
SCBA 15%	241.0	252.0	22.0	225.0	235.0	20.0
SCBA 20%	297.0	310.0	26.0	293.0	302.5	19.0
SCBA 30%	355.0	370.0	30.0	349.0	355.0	12.0

Fluid loss results data

Table A.5 Fluid loss for mixed ratios with FLYA

Mixed wt%	Room temperature Fluid loss (cc)	80°C Fluid loss (cc)
FLYA 0%	98.00	86.00
FLYA 10%	97.50	71.00
FLYA 15%	101.00	67.50
FLYA 20%	103.00	63.50
FLYA 30%	107.50	56.00

Table A.6 Fluid loss for mixed ratios with POFA

Mixed wt%	Room temperature Fluid loss (cc)	80°C Fluid loss (cc)
POFA 0%	98.00	86.00
POFA 10%	95.30	81.00
POFA 15%	91.00	74.80
POFA 20%	87.80	59.00
POFA 30%	82.50	46.50

Table A.7 Fluid loss for mixed ratios with SCBA

Mixed wt%	Room temperature Fluid loss (cc)	80°C Fluid loss (cc)
SCBA 0%	98.00	86.00
SCBA 10%	75.50	62.00
SCBA 15%	73.50	59.00
SCBA 20%	63.00	58.00
SCBA 30%	56.00	55.00

Thickening (setting) times results data

Table A.8 Thickening (setting) times for mixed ratios with FLYA

Mixed wt%	Initial setting time (hour)	Formation (mm)	Final setting time (hour)
FLYA 0%	4.5	9.0	8.0
FLYA 10%	5.0	7.0	9.0
FLYA 15 %	5.5	4.0	10.0
FLYA 20%	5.5	4.0	10.5
FLYA 30%	6.5	2.0	11.0

Table A.9 Thickening (setting) times for mixed ratios with POFA

Mixed wt%	Initial setting time (hour)	Formation (mm)	Final setting time (hour)
POFA 0%	4.5	9.0	8.0
POFA 10%	7.5	1.0	13.0
POFA 15%	11.5	2.0	16.0
POFA 20%	13.0	2.0	18.0
POFA 30%	14.5	2.0	20.0

Table A.10 Thickening (setting) times for mixed ratios with SCBA

Mixed wt%	Initial setting time (hour)	Formation (mm)	Final setting time (hour)
SCBA 0%	4.5	9.0	8.0
SCBA 10%	4.5	7.0	9.6
SCBA 15%	4.5	3.0	10.0
SCBA 20%	4.0	1.0	10.0
SCBA 30%	4.0	1.0	10.5

Compressive strength results data

Table A.11 Compressive strength for mixed ratios with FLYA

Mixed	Room temperature (psi)			80°C (psi)		
wt%	7 day	28 day	50 day	7 day	28 day	50 day
FLYA 0%	3091.12	4720.99	5620.22	4628.82	4496.18	955.44
FLYA 10%	3091.12	4777.19	6182.25	4889.59	5058.20	730.63
FLYA 15%	3596.94	5901.23	6182.25	4372.53	5170.61	1124.04
FLYA 20%	5058.20	6126.04	7306.29	3967.88	5339.21	1236.45
FLYA 30%	3091.12	5339.21	5901.23	3351.90	3653.15	1039.74

Table A.12 Compressive strength for mixed ratios with POFA

Mixed	Room temperature (psi)			80°C (psi)		
wt%	7 day	28 day	50 day	7 day	28 day	50 day
POFA 0%	3091.12	4720.99	5620.22	4628.82	4496.18	955.44
POFA 10%	3105.17	4777.19	6182.25	4608.58	4439.98	1067.84
POFA 15%	3596.94	5002.00	6182.25	4559.69	4945.80	1067.84
POFA 20%	4565.87	5058.20	6463.26	4441.66	5170.61	1180.25
POFA 30%	3963.94	3653.15	3653.15	3667.76	3653.15	843.03

Table A.13 Compressive strength for mixed ratios with SCBA

Mixed wt%	Room temperature (psi)			80°C (psi)		
	7 day	28 day	50 day	7 day	28 day	50 day
SCBA 0%	3091.12	4720.99	5620.22	4628.82	4496.18	955.44
SCBA 10%	4271.37	5620.22	6182.25	4396.70	4608.58	843.03
SCBA 15%	5058.20	5620.22	6182.25	4116.25	4720.99	927.34
SCBA 20%	5133.51	5620.22	6182.25	4089.84	4720.99	702.53
SCBA 30%	3527.81	4215.17	5564.02	1978.88	3484.54	618.22

Permeability results data

Table A.14 Permeability for mixed ratios with FLYA at room temperature

Curing time	Mixed wt%	D	H	Low Pressure, P =20	Low Pressure, P =10	High Pressure, P =20	High Pressure, P =10
		mm	mm	milidarcy	milidarcy	milidarcy	milidarcy
7 Day	0%	41.76	55.46	0.1310	0.1985	0.0239	0.0393
	10%	41.48	54.12	0.1134	0.1460	0.0187	0.0289
	15%	41.00	53.48	0.1052	0.1252	0.0117	0.0180
	20%	41.40	54.30	0.0939	0.1175	0.0094	0.0105
	30%	41.40	53.90	0.0752	0.0912	0.0069	0.0079
28 Day	0%	41.78	54.22	0.0912	0.1142	0.0159	0.0239
	10%	41.50	54.48	0.0854	0.1050	0.0112	0.0134
	15%	41.70	53.17	0.0818	0.0910	0.0092	0.0115
	20%	41.50	54.01	0.0753	0.0857	0.0061	0.0087
	30%	41.48	54.50	0.0655	0.0797	0.0045	0.0067
50 Day	0%	41.66	55.38	0.0802	0.1001	0.0108	0.0162
	10%	41.60	54.22	0.0781	0.0827	0.0084	0.0106
	15%	41.74	52.64	0.0636	0.0780	0.0043	0.0731
	20%	41.70	53.70	0.0473	0.0660	0.0024	0.0049
	30%	41.48	54.50	0.0359	0.0469	0.0017	0.0029

Table A.15 Permeability for mixed ratios with FLYA at 80°C

Curing time	Mixed wt%	D	H	Low Pressure, P =20	Low Pressure, P =10	High Pressure, P =20	High Pressure, P =10
		mm	mm	milidarcy	milidarcy	milidarcy	milidarcy
7 Day	0%	41.50	56.00	0.0719	0.1084	0.0246	0.0475
	10%	41.32	54.50	0.0573	0.0605	0.0162	0.0318
	15%	41.50	54.50	0.0266	0.0403	0.0095	0.0224
	20%	41.38	53.84	0.0139	0.0210	0.0082	0.0136
	30%	41.40	54.80	0.0107	0.0157	0.0065	0.0082
28 Day	0%	41.80	56.86	0.0145	0.0177	0.0031	0.0063
	10%	41.48	52.26	0.0101	0.0152	0.0028	0.0054
	15%	41.80	50.54	0.0072	0.0088	0.0013	0.0033
	20%	41.72	52.86	0.0038	0.0050	0.0011	0.0030
	30%	41.72	51.42	0.0025	0.0037	0.0011	0.0029
50 Day	0%	41.32	56.00	0.0102	0.0143	0.0028	0.0045
	10%	41.22	56.08	0.0091	0.0127	0.0015	0.0027
	15%	41.66	53.60	0.0056	0.0095	0.0008	0.0010
	20%	41.72	52.40	0.0022	0.0048	0.0004	0.0005
	30%	41.18	54.32	0.0016	0.0023	0.0001	0.0002

Table A16 Permeability for mixed ratios with POFA at room temperature

Curing time	Mixed wt%	D	H	Low Pressure, P =20	Low Pressure, P =10	High Pressure, P =20	High Pressure, P =10
		mm	mm	milidarcy	milidarcy	milidarcy	milidarcy
7 Day	0%	41.76	55.46	0.1310	0.1985	0.0239	0.0393
	10%	41.32	55.18	0.1046	0.1803	0.0180	0.0256
	15%	41.38	53.14	0.0829	0.1042	0.0104	0.0194
	20%	41.18	53.74	0.0521	0.0604	0.0089	0.0158
	30%	41.24	55.00	0.0338	0.0492	0.0078	0.0128
28 Day	0%	41.78	54.22	0.0912	0.1042	0.0159	0.0348
	10%	41.28	53.34	0.0807	0.0945	0.0120	0.0256
	15%	41.32	53.86	0.0497	0.0670	0.0091	0.0147
	20%	41.52	52.70	0.0402	0.0519	0.0083	0.0096
	30%	41.34	53.80	0.0297	0.0382	0.0046	0.0086
50 Day	0%	41.66	55.38	0.0802	0.1001	0.0108	0.0263
	10%	41.28	53.90	0.0285	0.0422	0.0083	0.0190
	15%	41.10	55.40	0.0190	0.0213	0.0046	0.0109
	20%	40.90	53.72	0.0078	0.0109	0.0022	0.0079
	30%	41.28	53.34	0.0035	0.0051	0.0010	0.0021

Table A17 Permeability for mixed ratios with POFA at 80°C

Curing time	Mixed wt%	D	H	Low Pressure, P =20	Low Pressure, P =10	High Pressure, P =20	High Pressure, P =10
		mm	mm	milidarcy	milidarcy	milidarcy	milidarcy
7 Day	0%	41.50	57.04	0.0719	0.1084	0.0246	0.0475
	10%	41.38	53.46	0.0648	0.0926	0.0204	0.0339
	15%	41.38	52.76	0.0411	0.0716	0.0193	0.0312
	20%	41.72	52.86	0.0364	0.0499	0.0136	0.0287
	30%	441.28	53.90	0.0226	0.0319	0.0059	0.0124
28 Day	0%	41.80	56.86	0.0145	0.0177	0.0031	0.0063
	10%	41.70	52.68	0.0097	0.0118	0.0027	0.0052
	15%	41.52	52.38	0.0083	0.0099	0.0021	0.0049
	20%	41.50	52.38	0.0078	0.0086	0.0018	0.0034
	30%	41.52	52.40	0.0061	0.0073	0.0011	0.0028
50 Day	0%	41.32	56.00	0.0102	0.0143	0.0028	0.0045
	10%	41.38	55.18	0.0059	0.0065	0.0024	0.0037
	15%	41.38	55.74	0.0037	0.0052	0.0019	0.0021
	20%	41.28	52.80	0.0024	0.0031	0.0014	0.0018
	30%	41.70	54.50	0.0017	0.0023	0.0007	0.0012

Table A18 Permeability for mixed ratios with SCBA at room temperature

Curing time	Mixed wt%	D	H	Low Pressure, P =20	Low Pressure, P =10	High Pressure, P =20	High Pressure, P =10
		mm	mm	milidarcy	milidarcy	milidarcy	milidarcy
7 Day	0%	41.76	55.46	0.1310	0.1985	0.0239	0.0393
	10%	41.80	55.30	0.0975	0.1308	0.0175	0.0295
	15%	41.54	56.94	0.0683	0.0945	0.0151	0.0241
	20%	41.50	56.20	0.0570	0.0883	0.0102	0.0177
	30%	41.48	55.62	0.0484	0.0710	0.0094	0.0160
28 Day	0%	41.78	54.22	0.0912	0.1042	0.0159	0.0348
	10%	41.40	55.20	0.0796	0.0962	0.0119	0.0282
	15%	41.50	55.40	0.0623	0.0840	0.0099	0.0143
	20%	41.18	55.60	0.0523	0.0767	0.0081	0.0112
	30%	41.30	55.28	0.0450	0.0593	0.0051	0.0068
50 Day	0%	41.66	55.38	0.0802	0.1001	0.0108	0.0263
	10%	41.30	56.88	0.0643	0.0749	0.0098	0.0248
	15%	40.98	55.10	0.0406	0.0669	0.0068	0.0126
	20%	41.42	55.92	0.0343	0.0416	0.0030	0.0059
	30%	41.10	54.62	0.0217	0.0348	0.0015	0.0048

Table A19 Permeability for mixed ratios with SCBA at 80°C

Curing time	Mixed wt%	D	H	Low Pressure, P =20	Low Pressure, P =10	High Pressure, P =20	High Pressure, P =10
		mm	mm	milidarcy	milidarcy	milidarcy	milidarcy
7 Day	0%	41.50	57.04	0.0719	0.1084	0.0246	0.0475
	10%	41.48	56.88	0.0659	0.0999	0.0218	0.0388
	15%	41.50	56.28	0.0540	0.0874	0.0186	0.0229
	20%	41.38	56.10	0.0459	0.0717	0.0124	0.0134
	30%	41.46	55.80	0.0375	0.0616	0.0091	0.0096
28 Day	0%	41.80	56.86	0.0145	0.0177	0.0031	0.0063
	10%	41.40	55.60	0.0117	0.0144	0.0029	0.0052
	15%	41.60	54.86	0.0092	0.0135	0.0025	0.0046
	20%	41.50	56.00	0.0061	0.0099	0.0021	0.0037
	30%	41.00	55.90	0.0056	0.0069	0.0013	0.0021
50 Day	0%	41.32	56.00	0.0102	0.0143	0.0028	0.0045
	10%	41.30	56.14	0.0100	0.0106	0.0026	0.0039
	15%	41.58	55.24	0.0083	0.0091	0.0019	0.0025
	20%	41.82	56.80	0.0042	0.0049	0.0006	0.0015
	30%	41.62	55.60	0.0019	0.0026	0.0001	0.0006

BIOGRAPHY

Mr. Watcharakon Setwong was born on May 20, 1991 in Buriram province, Thailand. He received his Bachelor's degree in Geotechnology from Institute of Engineering, Suranaree University of Technology (SUT) in 2013. For his post graduate, he continued to study for Master's degree in the school of Geotechnology, Institute of Engineering at SUT with the major in Petroleum Engineering. During graduation, 2014-2016, he served in position of teacher and research assistant at SUT. Since 2014, he has been a part-time teacher laboratory at SUT.